

IET Renewable Power Generation

Special Issue Call for Papers

**Be Seen. Be Cited.
Submit your work to a new
IET special issue**

Connect with researchers and
experts in your field and
share knowledge.

Be part of the latest research
trends, faster.

[Read more](#)



The Institution of
Engineering and Technology

ORIGINAL RESEARCH

Highly sensitive multifunction protection coordination scheme for improved reliability of power systems with distributed generation (PVs)

Feras Alasali¹  | Naser El-Naily² | Abdelaziz Salah Saidi³ | Awni Itradat⁴ | William Holderbaum⁵ | Faisal A. Mohamed⁶

¹Department of Electrical Engineering, Faculty of Engineering, The Hashemite University, Zarqa, Jordan

²Electric Technology, College of Electrical and Electronics Technology-Benghazi, Benghazi, Libya

³Electrical Engineering Department, College of Engineering, King Khalid University, Abha, Saudi Arabia

⁴Department of Computer Engineering, Faculty of Engineering, The Hashemite University, Zarqa, Jordan

⁵School of Science, Engineering and Environment, University of Salford, Salford, UK

⁶Science and Technology, Libyan Authority for Scientific Research, Tripoli, Libya

Correspondence

Feras Alasali, Department of Electrical Engineering, Faculty of Engineering, The Hashemite University, P.O. Box 330127, Zarqa 13133, Jordan.
Email: ferasasali@hu.edu.jo

William Holderbaum, School of Science, Engineering and Environment, University of Salford, Salford M5 4WT, UK.
Email: wholderbaum@salford.ac.uk

Funding information

King Khalid University, Grant/Award Number: RGP2/81/44

Abstract

The high penetration of distribution generators (DGs), such as photovoltaic (PV), has made optimal overcurrent coordination a major concern for power protection. In the literature, the conventional single or multi-objective function (OF) for phase overcurrent relays (OCRs) scheme faces challenges in terms of stability, sensitivity, and selectivity to handle the integration of DGs and ground fault scenarios. In this work, a new optimal OCR coordination scheme has been developed as a multifunction scheme for phase and ground events using standard and non-standard tripping characteristics. This research introduces and validates a coordinated optimum strategy based on two new optimization approaches, the Tug of War Optimization algorithm (TWO) and the Charged System Search algorithm (CSS), to mitigate the effects of DGs on fault currents and locations across the power network. Industrial software is used to create a case study of a CIGRE power network equipped with two 10 MW PV systems, and the results of the proposed new optimum coordination scheme are compared to traditional schemes. The findings show that the proposed multifunction OCR scheme is able to reduce the tripping time of OCRs over different fault and grid operation scenarios and increase the sensitivity of the relays in islanding operation mode.

1 | INTRODUCTION

Overcurrent relays (OCRs) are frequently used as an economic protection system for the main protection of sub-transmission and distribution systems, or multi-source to detect and isolate faulty elements. Coordination of OCRs is required to ensure that only the faulty network component is disconnected, and is intended to result in settings that provide the optimal operation sequence of the primary and backup relays for each protected

zone with a sufficient coordination time interval (CTI) margin [1]. Recently, numerous difficulties have arisen in OCRs coordination activities as a result of the integration of distribution generators (DGs). Because of the widespread adoption of DGs and two-directional power flow and fault characteristics have changed.

It has caused significant mis operational relay conditions and protection blinding by interfering with the selectivity and coordination of protective relays. In order to reduce the number

This is an open access article under the terms of the [Creative Commons Attribution-NonCommercial-NoDerivs](https://creativecommons.org/licenses/by-nc-nd/4.0/) License, which permits use and distribution in any medium, provided the original work is properly cited, the use is non-commercial and no modifications or adaptations are made.

© 2023 The Authors. *IET Renewable Power Generation* published by John Wiley & Sons Ltd on behalf of The Institution of Engineering and Technology.

TABLE 1 Optimal overcurrent relays coordination approaches for a power network with Distribution Generators.

Ref. no.	Year	Single objective	Multiple objective	Optimization technique	Conventional relay settings	Phase relay	Ground relay	Groups setting for ground and phase OCR
[4]	1996	P	O	GA	Conventional	P	O	O
[5]	1999	P	O	EP	Conventional	P	O	O
[6]	2006	P	O	SQP	Conventional	P	O	O
[7]	2008	P	O	GA	Conventional	P	O	O
[8]	2010	P	O	GA	Conventional	P	O	O
[9]	2011	P	O	GA	Conventional	P	O	O
[10]	2013	P	O	TLBO	Conventional	P	O	O
[11]	2015	P	O	PSA	Conventional	P	O	O
[12]	2016	P	P	MFA	Conventional	P	O	O
[13]	2016	P	O	IPM	Conventional	P	O	O
[14]	2015	P	O	NSGA-II	Conventional	P	O	O
[15]	2016	P	O	FBGA	Conventional	P	O	O
[16]	2017	P	O	PSO	Conventional	P	O	O
[17]	2018	P	P	MOPSO/FDMT	Conventional	P	O	O
[18]	2018	P	O	GA	Conventional	P	O	O
[19]	2018	P	O	IWO	Non-conventional	P	O	O
[20]	2018	P	O	DEA	Non-conventional	P	O	O
[21]	2018	P	P	NSGA-II	Conventional	P	O	O
[22]	2019	P	P	DE/LP	Conventional	P	O	O
[23]	2019	P	P	ESA-DEMO	Conventional	P	O	O
[24]	2019	P	P	GWO	Conventional	P	O	O
[25]	2019	P	P	FAGAM	Conventional	P	O	O
[26]	2020	P	O	ER-WCA	Non-conventional	P	O	O
[27]	2020	P	P	GA-LP	Conventional	P	O	O
[28]	2021	P	O	GA	Non-conventional	O	P	O
[29]	2021	P	O	MRFO	Conventional	P	O	O
[30]	2021	P	O	GA	Conventional	P	O	O
[31]	2021	P	P	NSGA-II-MILP	Conventional	P	O	O
[32]	2022	P	P	GA	Non-conventional	P	O	O
[33]	2023	P	O	GA-PSO-LP	Non-conventional	P	O	O
[34]	2023	P	P	MO-SSA-LP	Non-conventional	P	O	O

P: included; O : Not included.

of failures in protection coordination that occur in distribution networks (DN) as a result of new fault levels and the protection complexity given by DGs, OCR coordination is stated as an optimization problem with the objective of minimizing the relay's tripping time by determining its optimal setting [1–3]. In the literature, researchers have described several optimization strategies to determine the optimal OCR settings. Commonly, single objective function (OF) methods are typically used to coordinate overcurrent relays based on minimizing the total tripping time of OCRs. As indicated, the traditional single-OF is based on only one fault scenario, which is mainly the maximum fault scenario [4–7], as presented in Table 1. In the last few years, heuristic optimization approaches have emerged as viable tool for addressing the complexity of OCR coordination [8–34].

For example, these techniques include the genetic algorithm (GA) [7–9], particle swarm optimization (PSO) [16], sequential quadratic programming (SQP) [6], and hybrid optimization methods [23, 31, 34]. The single-OF, well-known and widely used in OCRs, seeks to be built and developed to give a rapid response, selectivity, and dependability to a faulty power network [4–7, 15]. However, this approach does not account for the significant effect that DGs have on the power protection system over different fault scenarios, and the optimal setting needs to cover primary and backup relays and different fault types, locations, and magnitudes. Now, in order to accomplish the most efficient protection scheme possible with OCRs in a DN with DGs, the protection coordination problem is formulated as a multi-objective (MO) optimization problem in such a way that it

minimizes the tripping time for both primary relays and backup relays that are required to operate [24, 27]. Table 1 outlines the key features of the research conducted on OCR coordination for DN equipped with DGs. In general, the literature on the formulation of OCR coordination settings using multi-objective optimization is limited. The studies [24, 27, 25, 23] focused on formulating the OCR coordination problem to minimize both the primary and backup phase OCR operating times for all possible primary-backup combinations simultaneously. In the multi-objective formulation that has been proposed, the maximum fault current is mainly considered to test and evaluate the proposed approaches [24, 28].

Most of the recent multi-objective coordination schemes for phase OCRs are formed with two major objectives based on minimizing the tripping time for both the primary and the backup, with different weighting factors assigned to each sub-objective [25]. To avoid miscoordination events, researchers added constraint conditions to the multi-OF, such as minimizing the coordination time interval (CTI) or CTI error [24, 28] or modifying the constraint priority [25]. For example, the authors in [24] developed a multi-OF for Phase OCR based on three subs OF: primary and backup relays tripping time and the CTI error and then solved it by using an evolution algorithm (GWO). In [27], two sub-OFs are proposed to be solved by GA-LP; the first OF is to describe the total tripping time for all relays and the second is to satisfy coordination constraints. However, the literature, as shown in Table 1, concentrated on developing a multi-OF for the Phase OCR protection scheme for specific fault conditions, primarily maximum faults, without taking into account the optimal setting across different fault types, locations, and magnitudes. For example, the strategies that were suggested in [24, 25] were not appropriate for the minimum fault current and line-ground and line-line-ground faults. Furthermore, the OCR coordination mechanisms in [31] did not address or account for the stochasticity of the DGs and instead relied mainly on the standard characteristic curves.

In a typical power protection system for a DN, the focus is primarily on identifying LLL fault (three phase fault) for developing phase OCR scheme and LG (line-to-ground) fault on implementing ground OCR relays scheme. Existing literature [16, 22–27, 34] has predominantly addressed the coordination challenge concerning Phase OCRs, neglecting the consideration of multiple operating functions (multi-OF) for ground OCRs when dealing with ground faults or coordinating between phase and ground OCRs. Detecting changes in fault currents resulting from different fault types is generally challenging when relying on the conventional method. Therefore, in this work, a new multi-OF for optimal OCRs coordination scheme is presented, considering the tripping time for phase and ground OCR as subs OFs and using standard and non-standard curves, respectively. The characteristic of the non-standard curve for the OCR function is intended to improve the performance of OCR protection compared to traditional schemes as used in [3, 16]. In addition, new robust metaheuristic optimization approaches, namely tug of war optimization algorithm (TWO) and charged system search algorithm (CSS), are employed to improve the OCR's protection performance in terms of sensitivity and selec-

tivity for both ground and phase OCR scenarios compared to standard and common algorithm in the literature (PSO) [16]. In this work, several tests will be conducted on a CIGRE benchmark microgrid while considering various fault scenarios to evaluate the proposed protection approach.

1.1 | Contributions

It is clear from the aforementioned evidence that the nature of DGs in power networks will necessitate an OCR protection mechanism that is more advanced than what is used in the literature. OCR protection schemes must be compatible with different fault scenarios and characteristics. These challenges encountered with the conventional single-OF or multi-OF for OCR scheme raise concerns about the appropriateness of the practiced characteristics in terms of stability, sensitivity, and selectivity. This research introduces a new multi-OF for optimal coordination of both phase and ground OCRs in a power network based on standard and non-standard time-current curves, respectively, for fast-response OCRs in DN with DGs. To reduce the OCRs response time over line-ground and three-phase fault conditions as subs OFs and improve the protection scheme effectiveness, the new TWO and CSS algorithms have been used and compared to PSO. The primary original contributions of this study are as follows:

- (i) A novel multi-OF for optimal OCRs coordination scheme is established, considering phase and ground OCR conditions as subs OFs to improve protection performance compared to single OF [4–7, 16] from the literature. A significant reduction in total operational time with no instances of miscoordination by using non-standard tripping characteristics for multi-OF schemes compared to conventional characteristics used in the literature.
- (ii) Employing two new robust metaheuristic optimization approaches, TWO and CSS, to improve protection performance compared to standard and common algorithm in the literature (PSO) [16].
- (iii) Finally, to give the DN operators a preliminary indicator regarding the potential impact of DGs such as PVs on the fault contribution and relay setting, a comparison analysis is performed for the new multi-OF coordination approaches under different fault scenarios in the CIGRE distribution network. In addition, since current measurements are collected locally, the proposed new multi-OF coordinating scheme does not require a communication channel between the OCRs. This is intended to reduce the need for communications infrastructure and computing costs.

1.2 | Outline of the paper

The rest of this work is organized as follows: the problem description and formulation of OCRs coordination are presented in Section 2. The proposed multifunction optimal

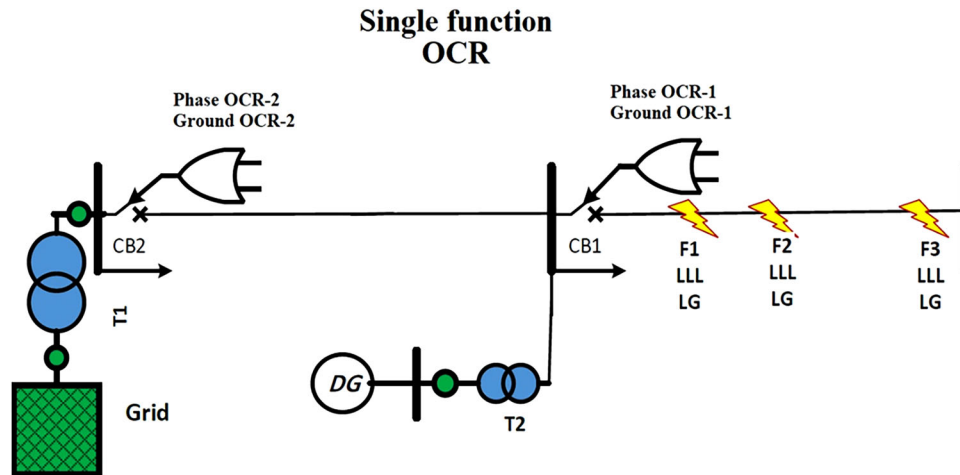


FIGURE 1 Single line diagram of the distribution networks with phase and ground overcurrent relays as single function relays.

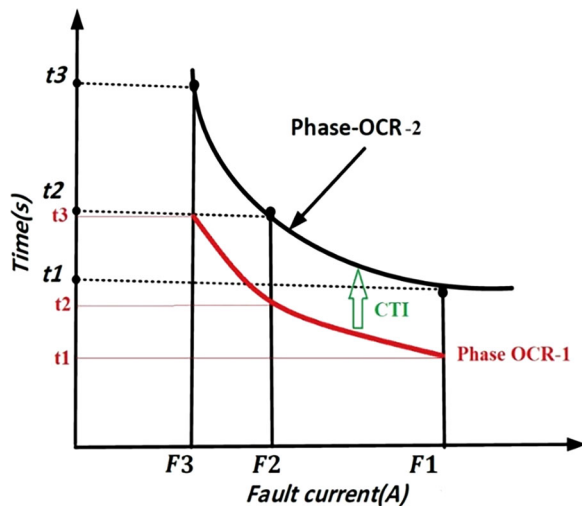


FIGURE 2 The conventional overcurrent relay characteristics.

protection scheme for phase and ground OCRs is illustrated in Section 3. Then Sections 4 and 5 present the simulation results analysis and conclusions of this work.

2 | PROBLEM DESCRIPTION AND FORMULATION OF STANDARD OCRS COORDINATION

Distribution networks (DNs) that incorporate DGs, including photovoltaic systems (PVs), must be adequately protected to ensure their continued safe and reliable operation. Overcurrent relays (OCR-1 and OCR-2) are shown protecting two power lines (L1 and L2) of the DN, as shown in Figure 1. The OCRs are coordinated based on a coordination time interval (CTI). Figure 2 shows the traditional coordination curves of phase OCRs for the DN. For instance, if a failure occurs at location F1, the primary and secondary relays for that location are OCR-1 and OCR-2, respectively. Due to the stochastic nature of DG, the minimum and maximum fault current levels fluctuate

widely, increasing the complexity of using standard protection schemes [2, 3]. The fault characteristics of a DN with and without DGs are different due to the changes in DN architecture, volatile load and generation levels, and different fault resistance. Various types of faults exist, including LLL, LL, LLLG, LLG and LG, where the LG is commonly known, is the most frequent electrical failure up to 85% of faults [2–4]. Typically, a fault analysis on a DN only offers information regarding LLL and LG faults. The first provides data for phase relaying (Phase OCR) while the second provides data for ground relays (ground OCRs). In practice, the other categories of faults are rarely required. The LG and LLL fault values will be different for DN with DG compared to the power network without DG, which could cause the OCR-2 to fail if a failure occurs on the OCR-1 and mis coordination events. In general, the literature [22, 25, 27] concentrated on introducing the coordination problem for phase OCRs while ignoring a multi-OF for ground OCRs with ground faults. Changes in fault currents caused by various types of faults are typically difficult to detect using the standard method. Therefore, in order to respond to the failure in all DG operation modes under different types of faults (phase and ground), it is necessary to build a new multi-OF scheme for OCR at DN with DG. In this research, the primary goal of developing new multi-OF coordination schemes using standard and non-standard tripping characteristics is to find the optimal time multiplier settings (TMS) for the coordination curves that will result in the minimum tripping time for the OCR under phase and ground faults scenarios.

2.1 | Formulation of a standard OCR coordination problem

In general, the coordination between the OCRs in the standard protection scheme is primarily determined under the assumption that the network parameters and fault conditions will not change. Equation (1) outlines the critical time interval (CTI) that exists between the primary and backup relays for a fault scenario, as shown in Figure 2. The CTI indicates that

TABLE 2 Common and recent optimal overcurrent relays coordination problems.

Ref.	Single or multi OF	Objective function
[4]	Single-OF	OF = $W \sum t_{back} - t_{prim}$
[5, 7]	Single-OF	OF = $(W_1 \sum t_{prim} + W_2 \sum t_{back})$
[6, 15]	Single-OF	OF = $W_1 \sum t_{prim}^2 + W_2 \sum (t_{back} - CTI)^2$
[26]	Single-OF	OF = $\sum_{earth\ phase} \sum t_{prim}$
[24, 27]	Multi-OF	OF1 = $W_1 \sum t_{prim}$ OF2 = $W_2 \sum t_{back}$ OF3 = $W_3 \sum CTI$
[25]	Multi-OF	OF1 = $W_1 \sum t_{prim}$ OF2 = $W_2 \sum t_{back}$
[34]	Multi-OF	OF1 = $\sum f_c$ OF2 = $(W_1 \sum t_{prim} + W_2 \sum t_{back})$

the coordination time between the primary (t_{prim}) and backup (t_{back}) relays ought to be equal to or higher than the CTI that has been defined between 0.2 and 0.5 s in [3]. The tripping time for the OCR, t , in standard protection schemes, is determined using Equations (2) and (3) based on the known value of the fault current, I_f , and the pickup current, I_{pick} [1]. In Equations (2) and (3), and are the fault and pickup current, respectively. The A, B, and C parameters are related to the type of OCR characteristics and standards, as discussed in detail in [1–3].

$$t_{back} - t_{prim} \geq CTI \quad (1)$$

$$t = \left[\frac{A}{\left(\frac{I_f}{I_{pick}} \right)^B - 1} \right] \text{TMS} \quad (2)$$

$$t = \left[\frac{A}{\left(\frac{I_f}{I_{pick}} \right)^B - 1} + C \right] \text{TMS} \quad (3)$$

In the literature, the OCRs coordination using standard schemes problem is presented as an optimization problem. The common and recent prevalence of the OCR coordination problem is shown in Table 2. The single-OF scheme has been described in [4–7, 15, 16, 26]. In [5–7], the authors aimed to minimize the total tripping time of all OCR (primary and backup relays), $\sum t_{prim}$ and $\sum t_{back}$ are the total tripping time of primary and backup OCRs, respectively, based on the use of weighted factors (W) for each OCR. The CTI error or constraints are added to the single-OP to improve the tripping time as in [6]. In 2020, the authors in [26] presented a single OF for minimizing the total tripping time of the primary earth and phase OCRs. However, the solution of the OF in [26] will lead to finding the optimal set of only primary OCR for both earth and phase OCRs at the same time, without considering the differ-

ent fault characteristics. On the other hand, the multi-OF for the coordination OCR problem is primarily composed of two major sub-OFs for reducing the tripping time of primary and backup OCR in the event of a specific fault [25]. Each sub OF has been weighted by factors (W) to present the priority for each sub OF. Recently, to avoid miscoordination events, researchers converted the constraint conditions to the multi-OF, such as minimizing the coordination time interval ($t_{back} - t_{prim}$) and the CTI error [24, 27], or minimizing the cost of using a fault current limiter, $\sum f_c$ [34]. However, adding DG to the DN leads to changes in fault characteristics, and it is necessary to build a new multi-OF scheme able to deal with different fault scenarios.

3 | PROPOSED METHOD: OPTIMAL MULTIFUNCTION PROTECTION SCHEME FOR PHASE AND GROUND OCR

By including DGs in the DN, the fault current travelling through the primary and backup relays has new fault levels. The goal of OCR coordination between primary and backup relays is to determine the optimal TMSs to minimize the travel time of the OCRs. In the literature, the typically inverse time–current characteristics have been utilized, as described in Equations (2) and (3) by [1–3]. However, these standard curves are restricted to certain setting values of low and high TMS, which reduce the sensitivity of OCR at the new fault level and different types of faults in DN with DGs [35]. Consequently, standard protection schemes cannot be employed to solve the relay coordination problem under all fault conditions, and a new scheme must be implemented.

To minimize the limitation in the inverse time-current characteristics and protection difficulties for DG systems, this paper presents an enhanced new OCRs coordination strategy based on a multifunction OCR based on the multi-OF formulation for ground and phase OCRs underground and phase faults by using non-standard and standard tripping characteristics. Figure 3 depicts the proposed optimal multifunction coordination strategy for OCRs that will be utilized in this article. First, a CIGRE power network (14-bus) is created by using ETAP simulation, and then load flow analysis and short circuit calculation are performed using the Newton–Raphson algorithm based on IEC60909. Then, the optimal setting for each sub OF is obtained, TMS for phase OCR (TMSP) and TMS for ground OCR (TMSG), by employing the CSS and TWO algorithms to solve the multi-OF. The CSS and TWO algorithms are implemented in MATLAB for this study. The results of the multi-OF approaches will be compared with the single-OF approach in terms of CTI constraint and total tripping time. The optimal OCR settings acquired from MATLAB were validated using ETAP software under various fault scenarios. Finally, the proposed multi-OF protection scheme is tested in different DN operation scenarios. In the following section, the multi-OF protection scheme based on non-standard tripping characteristics is introduced.

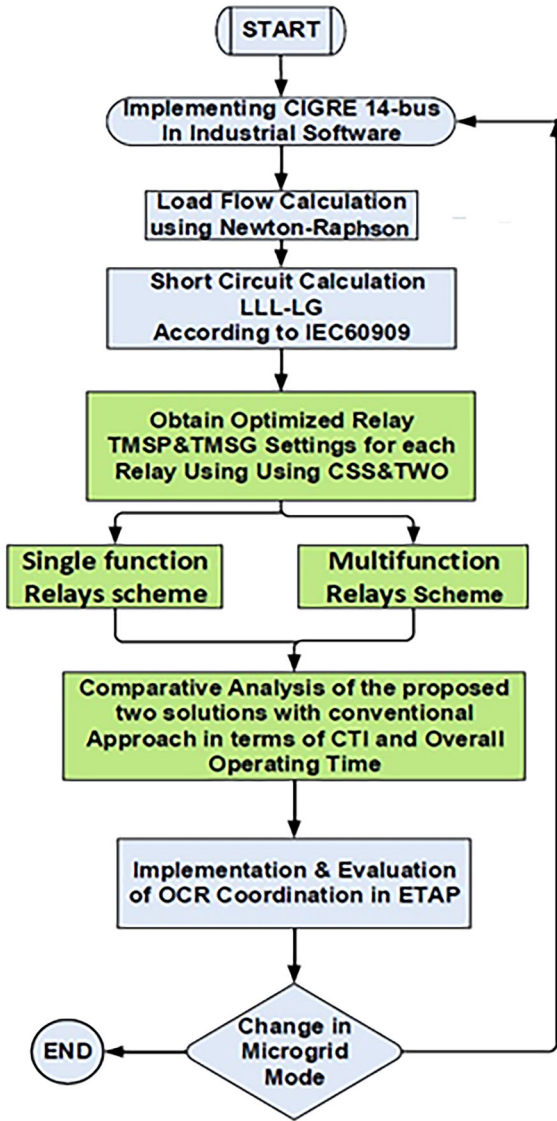


FIGURE 3 A workflow of the proposed multifunction optimal overcurrent relays coordination scheme implemented in this work for different microgrid modes (with and without distribution generators and islanding).

3.1 | Proposed coordination problem formulation

This paper uses a mathematical multi-OOF optimization model to describe the OCRs coordination problem in a DG equipped with DN. Recently, the OCR can be designed and operated with multifunction schemes. Therefore, this work aims to develop a new multifunction OCR coordination scheme to minimize the tripping time of phase and ground faults scenarios. The multi-objective function (multi-OF) includes two subs OFs for the total tripping time of all OCRs, where OF1 is the sub function for phase OCR function (phase fault scenario) and OF2 is the sub-function for ground OCR (ground fault scenario), described in Equation (4). The multi-OF for the total number of OCRs, K , and the total fault location, L , is described as

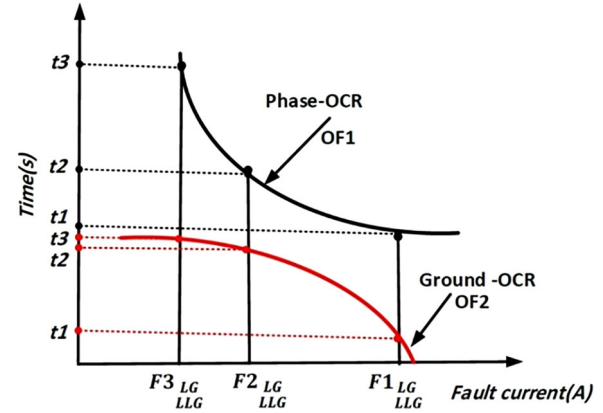


FIGURE 4 The non-standard and standard tripping characteristics for phase and ground overcurrent relay as multifunction relays.

follows:

$$\text{multi-OF} \begin{cases} \text{OF1} = \sum_{k=1}^K \sum_{l=1}^L t_{p, k, l} \\ \text{OF2} = \sum_{k=1}^K \sum_{l=1}^L t_{g, k, l} \end{cases} \quad (4)$$

This will help to find the optimal OCR setting to minimize the total tripping time; tripping time under different faults for the primary and backup relays. Finding the optimal OCRs setting (TMS) that minimizes the operational time of OCRs without sacrificing selectivity between primary and backup relays is the primary focus of the proposed optimization formulation. Therefore, non-standard tripping characteristics are used in this work to determine the tripping time, t_g , and find the TMSG at OF2. In general, the non-standard tripping characteristic is basically a logarithmic function of the tripping time based on the fault current, as described in Equation (5) and Figure 4. Many studies [1, 3] use non-standard characteristics to coordinate OCR, especially those based on a single-OF. This has the potential to improve OCR coordination under various fault scenarios based on multi-OF. Furthermore, programmable or numerical OCR can use a variety of standard and non-standard curves, as well as user-defined functionality [1, 3]. For phase fault scenarios (OF1), the standard tripping characteristic is employed to determine the tripping time, t_p , and find the TMS, as shown in Figure 4 and described by Equation (6).

$$t_g = \left(5.8 - 1.35 \log_c \left(\frac{I_f}{I_{pick}} \right) \right) \text{TMSG} \quad (5)$$

$$t_p = \left[\frac{A}{\left(\frac{I_f}{I_{pick}} \right)^B - 1} \right] \text{TMSG} \quad (6)$$

The proposed multi-OF scheme based on non-standard time-current characteristics will consider the impact of fault location, type, and value to improve the selectivity and sensitivity of the protection system. In addition, the non-standard characteristic will provide a sufficient area to detect the different faults (minimum and maximum), as shown in Figure 4. Consequently, the coordination based on the multi-OF scheme and non-standard characteristic will result in optimal grading time relative to the relay operation time. The multi-OF presented in (4) is subjected to protection and network constraints.

- Firstly, the selectivity and coordination constraint in Equation (1) imposes a propositional time delay (CTI) between the primary and backup OCRs. This producer will assist in minimizing network power interruptions according to the location of the fault, and backup OCRs operating only if the primary OCRs do not run [1].
- Secondly, the limits of relay operating time and setting aim to maintain the operational time for relay n , t_n , and relay setting, TMS_n , within minimum and maximum limits, as presented in Equations (7) and (8) [2, 3]. TMS is handled as a continuous variable in this work for both functions (ground and phase).

$$t_{min} \leq t_n \leq t_{max} \quad (7)$$

$$TMS_{min} \leq TMS_n \leq TMS_{max} \quad (8)$$

Figure 5 shows the workflow of the proposed multifunction OCRs approach. The proposed multifunction OCRs approach is made up of a number of parts that are used in the different fault scenarios (ground or phase). The current sequence block (abc/012) receives the current measurements from the CTs' to generate a current sequence output in proportion to the input. If the output of the current sequence block (abc/012) includes zero-sequence current components (I0), the OF2 as ground OCR will handle the fault. Otherwise, the fault will be handled by OF1 as phase OCR. In the output value of the OCR on the OF2, pickup ground and TMSG will be rectified using the non-standard curve in Equation (5). Then, the ground trip block will send a tripping signal to the multifunction OCR (MFOCR 1). In the case of phase OCR, the OF1, as described in Equation (6), calculates the pickup phase OCR output and TMSF values and sends the trip signal to the (MFOCR 1). This process and the logic of the proposed multifunction scheme aim to minimize the total tripping time of the OCR at different fault conditions (phase and ground scenarios). The coordination of multifunction OCRs, for example, MFOCR 1 and MFOCR 2 is part of the coordination process in this work by applying the constrainers in Equations (6) and (7). In this work, the fault location considered is indeed identical to the test 12 different fault locations which cover the all main buses at the CIGRE 14 bus system. The purpose of selecting these specific fault locations was to evaluate and demonstrate the effectiveness of the proposed scheme under various scenarios.

3.2 | Optimization algorithms

By organizing the TMSP and TMSG of phase and ground function at the OCR in the proposed multi-OF, the tripping time of each OCR for different fault scenarios is computed by solving the multifunction optimization problem. In this study, the proposed multifunction protection approach ensures that the relay runs quickly based on the fault conditions. The proposed multifunction phase and ground OCR protection approach aim to the total tripping time over different fault scenarios while satisfying all DN and OCR coordination constraints between the MFOCRs. In this work, the tug of war optimization algorithm (TWO) and charged system search algorithm (CSS) [36] are used to solve the proposed multifunction optimization problem. The selection of these two modern optimization algorithms as powerful algorithms for solving complex problems and promising algorithms for handling complicated engineering problems, was based on their high performance in different benchmark and complex problems [36].

3.2.1 | Tug-of-war optimization algorithm (TWO)

A novel population-based metaheuristic algorithm was created by Kaveh and Zolghadr [36] who drew their inspiration from the game of tug of war. The TWO algorithm, in contrast to the majority of other metaheuristic approaches, is formulated in such a way that it takes into account the characteristics of the interacting solutions. The TWO algorithms can be used for complex problems with non-smooth and non-convex behaviour. Figure 6 shows the general concepts and framework of the TWO algorithm as described in detail in [36]. Firstly, TWO generates its first set of potential solutions in a random solution. Each potential solution is set to be a different team. The system iteratively evaluates each team (solution) and gives them a weight that is directly related to how well they performed. The best solution (team) is given the most weight and the weakest team the least. Then, two solutions (teams) will rival, and, typically, the weaker team will lose and moves toward the stronger one based on the idealizing the tug of war framework and Newton's second law. Then, a random solution will be added to the formulation derived from Newton's laws. In every iteration, the population is revised and updated by the random solution to move outside the rest area and achieve the optimal solution. This process will be terminated if the maximum number of iterations or OF evaluations is achieved.

3.2.2 | Charged system search algorithm

Kaveh and Talatahari [36] created the charged system search (CSS) algorithm as a population-based metaheuristic by employing some concepts from physics and mechanics (Coulomb and the Newtonian laws) and was effectively applied to a variety of structural optimization problems. Table 3 presents the general

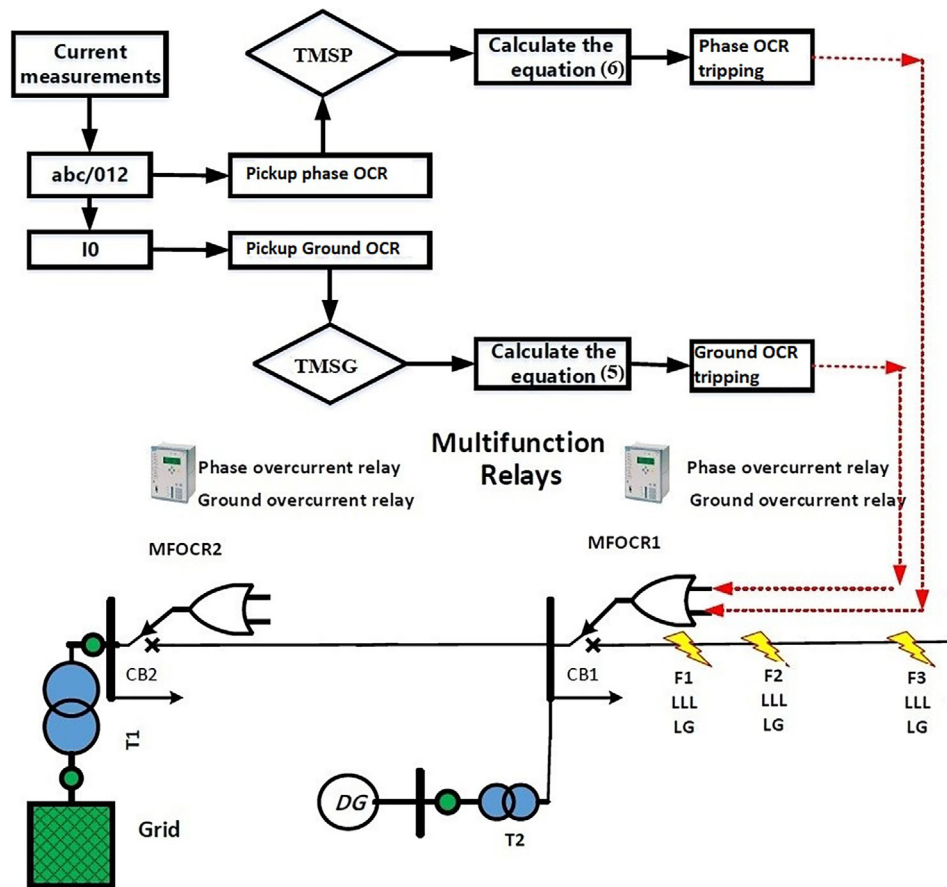


FIGURE 5 Schematic signal diagram of the proposed multifunction overcurrent relays.

concepts and framework of the CSS algorithm, as described in detail in [36]. Firstly, CSS initialize the problem and generates its first set of potential solutions at a random solution. Each candidate solution in the search space is a charged particle. Particles' charge and mass are inversely proportional to the value of their objective function, with higher values for both properties corresponding to lower values for the objective function. Throughout each iteration, transitions of particles can be generated based on the particle-to-particle electrostatic interactions. The purpose of these interactions is to attract or repel the particles in the direction of the optimal position. The rules of electrostatics and Newtonian mechanics, respectively, will be applied to conclude the magnitude of the resulting electric force and the nature of the movement.

4 | DESCRIPTION OF THE GRID-CONNECTED PV INVERTER SYSTEM

There has been a significant increase in interest among electrical energy producers and environmentalists in DGs such as PV systems [1]. These devices allow local electricity delivery, lowering reliance on the central power system and minimizing power loss. Furthermore, PVs units enable the autonomous operation of

localized electrical energy networks. Therefore, this section aims to describe the grid-connected PV inverter model used in this work and the impact of the fault current analysis of PV system.

4.1 | PV system model

This section presents the detailed configuration and operation of a grid-connected photovoltaic (PV) system used in this work, specifically utilizing a three-phase voltage source inverter (VSI). Illustrated in Figure 7, are the system's main components such as the PV array, MPPT and inverter. The PV array is connected to the boost converter, which is in turn linked to the inverter. To optimize the power extraction from the PV system, the boost converter and MPPT algorithm are employed, enabling the system to track and utilize the maximum available power. The three-phase VSI, along with its control system and RLC filter, is responsible for connecting the PV system to the low-voltage AC grid. This connection is facilitated through a step-up transformer on the distribution side, ensuring a seamless power supply to the load. The VSI system regulates the conversion and transfer of power from the PV system to the grid, enabling efficient utilization of the generated electricity [37].

The solar cell is the primary component of the PV system. A solar cell is capable of directly converting sunlight into

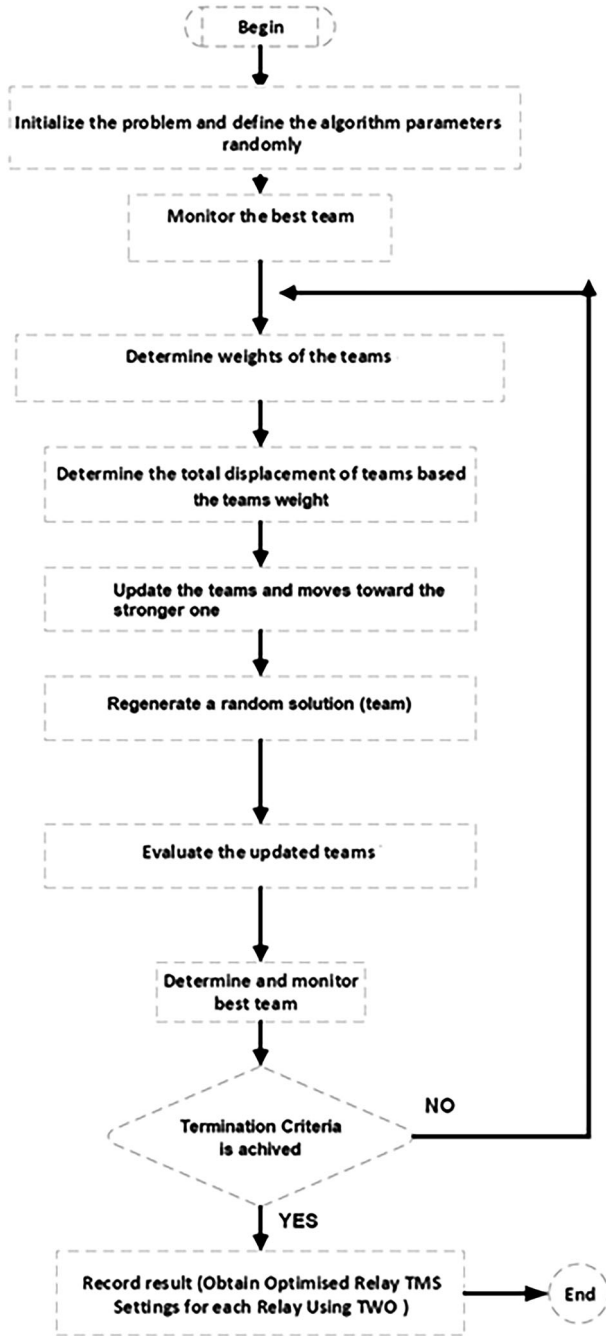


FIGURE 6 Flow chart of the tug-of-war optimization algorithm.

electricity. Multiple solar cells are typically connected in series to form a PV module [37, 38] to generate higher voltages and power levels. Commonly, the PV module's equivalent circuit, as shown in Figure 8, is used to depict its electrical behaviour. This circuit model is comprised of several essential components that represent the fundamental characteristics of the PV module. These elements consist of a current source representing the current generated by the solar cell, a diode representing the solar cell's intrinsic non-linear behaviour, a series resistance accounting for resistive losses, and a shunt resistance accounting for any parasitic shunt paths within the module. This enables the optimization of PV system design, the evaluation of sys-

TABLE 3 The charged system search algorithm procedures.

Steps	Description
Step 1: Initialize the population	<ul style="list-style-type: none"> Initializing the problem. Defining the algorithm parameters and the maximum number of iterations. Generating random solutions (charged particles).
Step 2: Population evaluation	<ul style="list-style-type: none"> Evaluating the solution and memorizing the best one. Determining the charged particles' magnitude, vector, and distance to move towards the optimal solution based on the particle-to-particle electrostatic interactions.
Step 3: Updating CSS search area	<ul style="list-style-type: none"> Regenerate the solutions (charged particles) by using the harmony search. Evaluating the new solutions and memorizing the best one.
Step 4: Terminating criterion	<ul style="list-style-type: none"> Since CSS is an iterative procedure, the aforementioned actions from 2 will be repeated until the maximum number of iterations has been reached.

tem performance, and the development of efficient control strategies.

A PV cell can be represented by a basic circuit model that includes a genuine diode connected in parallel with a theoretical current source. The theoretical current source produces a current that is directly related to the amount of solar radiation it receives. The relationship between the output voltage and current based on the equivalent circuit is expressed in the following equation [37]:

$$I_{pv} = I_{pb} - I_d - I_{sb} = I_{pb} - I_0 e^{\frac{V_{pv} + I_{pv} R_S}{n_s V_i Q_d}} - 1 - \frac{V_{pv} + I_{pv} R_S}{R_{Sb}} \quad (9)$$

where V_{pv} and I_{pv} are the voltage and current of the PV model, I_{pb} is the light current, I_d and Q_d are the current of and ideality factors of the diode, I_0 is the reverse saturation current of the diode, R_{Sb} and R_S are the shunt and series resistance, V_i is the thermal voltage. This section provides the main parameter values for the PV module and inverter unit used in this work for a 1 MW PV unit, which is outlined in Tables 4 and 5. These values are utilized in the mathematical model of the PV module discussed earlier and in [37, 38]. By incorporating these parameter values into the model, we can accurately simulate and analyse the behaviour and performance of the PV module under different operating conditions

4.2 | Fault current analysis of power network with PVs

The integration of DG units presents certain technical challenges for the operation of distribution networks. The intermittent nature of electricity production from PVs, influenced

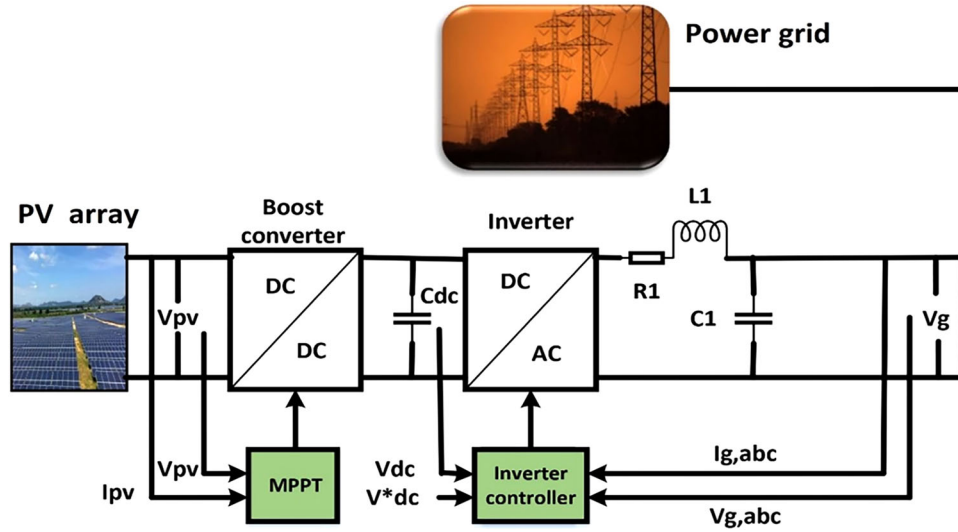


FIGURE 7 Schematic of the grid-connected photovoltaic system.

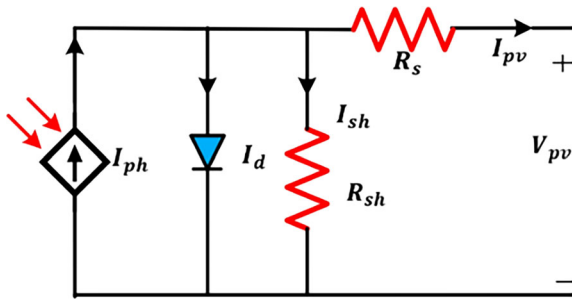


FIGURE 8 Equivalent circuit of the photovoltaic model.

TABLE 4 The key parameters of the photovoltaic module.

Parameters of the PV module	Value
Maximum power	$P_{max} = 235 \text{ W}$
Maximum power voltage	$V_{mp} = 29.3 \text{ V}$
Maximum power current	$I_{mp} = 7.68 \text{ A}$
Open-circuit voltage	$V_{oc} = 36.8 \text{ V}$
Short-circuit current	$I_{sc} = 8.2 \text{ A}$
Cell number per module	$N_s = 60$
Temperature coefficient of I_{sc}	$K_i = 0.062/^\circ\text{C}$
Temperature coefficient of V_{oc}	$K_v = -0.273/^\circ\text{C}$
Ideality factor of the diode	$Q_d = 0.95$

TABLE 5 The key parameters of the inverter connected grid.

Parameters of the inverter	Value
K_i	1.5 p.u.
T_i	0.01 s
K_d	1 p.u.
T_d	0.05 s
L_f	0.5 mH
The effective voltage of the grid	$V_{grid} = 66 \text{ KV}$
DC link voltage	$V_{dc} = 1800 \text{ V}$
DC link capacitor	$C_{dc} = 6000 \mu\text{F}$
Grid frequency	$\omega = 2\pi \times 50 \text{ rad/s}$
R filter of the inverter	$R_f = 10 \text{ m}\Omega$
L filter of the inverter	$L_f = 1.6 \text{ mH}$
Switching frequency of the inverter	$f_s = 3.25 \text{ kHz}$

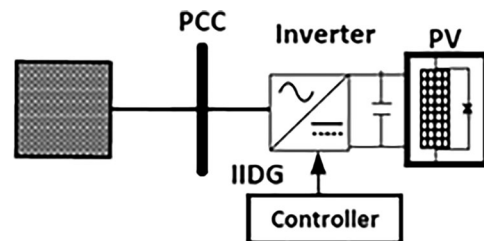


FIGURE 9 Equivalent circuit of inverter-interfaced distributed generation.

by environmental conditions, necessitates the distribution network operator to reassess the existing operation and protection mechanisms [2, 3]. The dependable and uninterrupted distribution of electrical energy to users should be prioritized in the design of an electrical network. Short-circuit failures are among the major threats to network integrity, and if not addressed, they can cause irreparable damage. As discussed in Sections 1 and 2, protective devices are put in the system to reduce these dangers, with OCRs being the most often used PDs in distribution networks. These devices are crucial in detecting and responding

to overcurrent problems promptly. The optimal selection and configuration of OCRs play a critical role in enhancing the reliability and security of the electrical network's protection system. Traditionally, the protection system of distribution networks has been designed based on the assumption of unidirectional power flow. However, the growing integration of PV units presents a significant challenge to the existing protection system. This is

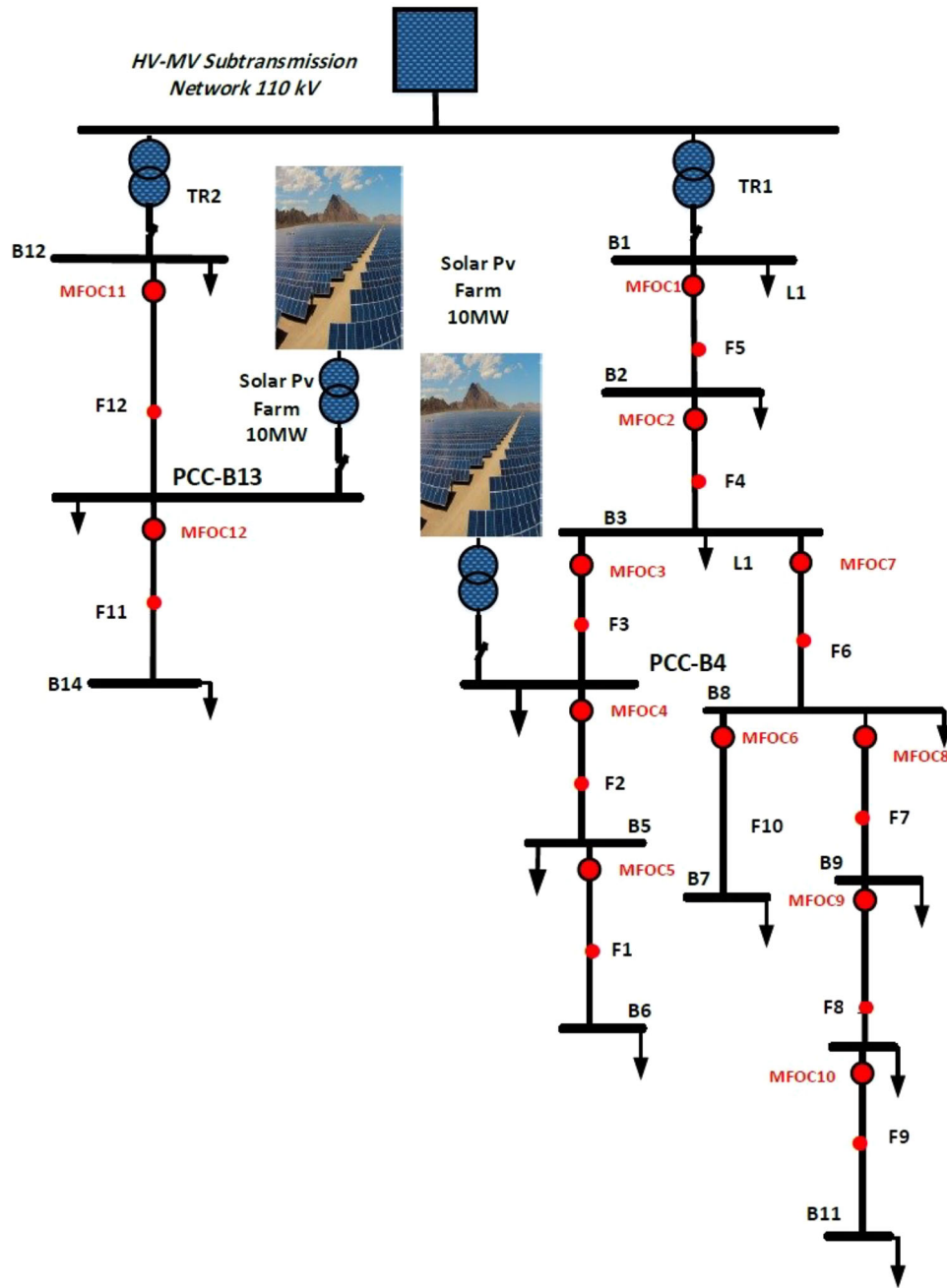


FIGURE 10 The modified 14-bus CIGRE system under study.

TABLE 6 The basic information of the multifunction overcurrent relay at the CIGRE network.

Relay	Current transformer ratio	OF1 (phase OCR)		OF2 (ground OCR)	
		Plug setting	Pickup current (I_{pick} , (A))	Plug setting	Pickup current (I_{pick} , (A))
MFOCR 1,2	200/1	60	120	20	40
MFOCR 3 to 6	100/1	50	50	20	20
MFOCR 7	100/1	60	60	20	20
MFOCR 8 to 12	100/1	50	50	20	20

TABLE 7 The multiplier settings values for objective functions (1) and (2), the multiplier settings for phase and ground overcurrent relay at the CIGRE network.

Relay	Scenario 1				Scenario 2				Scenario 3			
	TMSP		TMSG		TMSP		TMSG		TMSP		TMSG	
	TWO	CSS	TWO	CSS	TWO	CSS	TWO	CSS	TWO	CSS	TWO	CSS
MFOCR1	0.659	0.628	1.038	4.48	0.475	0.6	0.629	0.28	0.18	0.242	0.459	0.25
MFOCR2	0.445	0.462	0.375	2.57	0.338	0.45	0.176	0.19	0.137	0.18	0.158	0.18
MFOCR3	0.401	0.402	0.324	1.4	0.304	0.4	0.129	0.15	0.177	0.23	0.115	0.12
MFOCR4	0.201	0.19	0.17	0.55	0.159	0.21	0.093	0.42	0.112	0.14	0.08	0.14
MFOCR5	0.01	0.017	0.01	0.01	0.01	0.001	0.01	0.01	0.01	0.01	0.01	0.01
MFOCR6	0.455	0.035	0.301	0.01	0.01	0.04	1.15	0.098	0.038	0.01	86	0.01
MFOCR7	0.577	0.57	0.356	1.83	0.514	0.58	0.58	1.26	0.496	0.38	0.423	0.42
MFOCR8	0.412	0.394	0.256	1.09	0.338	0.41	0.355	0.79	0.343	0.28	0.217	0.28
MFOCR9	0.2	0.2	0.111	0.53	0.162	0.21	0.156	0.39	0.171	0.14	0.081	0.14
MFOCR10	0.01	0.01	0.01	0.01	0.01	0.01	0.025	0.01	0.041	0.01	0.01	0.01
MFOCR11	0.22	0.006	0.238	0.0105	0.059	0.01	0.011	0.01	0.0548	0.01	0.01	0.01
MFOCR12	0.474	0.17	0.452	0.0.16	0.45	0.23	0.461	0.1	0.321	0.11	0.066	0.07

due to variations in the magnitude and direction of fault currents caused by the presence of PV units. When PV units are integrated into a radial distribution network, multiple points become sources of power supply. Additionally, the behaviour of the PV units during faults and their impact on the magnitude and direction of short-circuit currents can differ significantly [1–4].

In general, the fault characteristics of voltage source inverters (VSI) based on inverter-interfaced distributed generation (IIDG) are primarily influenced by its control strategy, with PQ control being widely employed. The PQ is controlled by the current limits to ensure that the fault current of IIDG does not exceed twice its rated current. Moreover, IIDG is designed to have a low voltage ride-through capability, based on the grid code in [39], providing reactive power support to meet the grid requirements [38]. In Figure 9, IIDG is represented as a current source controlled by the positive sequence voltage at the point of common coupling (PCC). Thus, the magnitude of the IIDG fault current depends on the intermittent nature of the new energy source and is influenced by changes in the positive sequence voltage. During a fault, the PV plant operates under different control strategies, leading to various operating modes. These operating modes can result in the faulted phase current being smaller than the healthy phase currents. Therefore, selecting the faulted phase and developing a protection model with an optimal coordination scheme based on the magnitude of phase current becomes a challenging task.

5 | SIMULATION RESULTS AND DISCUSSION

In this section, the proposed optimal multifunction protection scheme for phase and ground OCRs and the coordination problem, as discussed in Section 3, is evaluated using a 14-bus DN

(CIGRE network). This article aims to test the proposed multifunction OCR scheme with different modes of operation of DN (islanding, with and without DGs). In addition, the proposed multifunction scheme with non-standard and standard tripping curves will be compared to single function relays and standard protection approaches. The description of DN (14-bus CIGRE network) is presented first, followed by the results of testing the proposed multifunction OCR scheme using a variety of power network models and fault conditions. This section compares the proposed multifunction OCR scheme to common and standard schemes in terms of total tripping time and CTI error events. The TWO and CSS algorithms are employed to solve the multifunction OCRs coordination problem using non-standard and standard time curves. Both the results of the TWO and CSS algorithms are analysed and contrasted in this section. The technique for multifunction OCRs has been evaluated using industrial software (ETAP), and the results are presented and compared to the standard approaches. The proposed multi-OF scheme is validated using GE Multilin, model-750/760 overcurrent relay (AREVA, P139) in ETAP.

5.1 | Description of the DN

The proposed optimal multifunction protection scheme for phase and ground OCRs (MFOCR) is evaluated on a CIGRE network, as depicted in Figure 10, to determine the optimal setting for MFOCRs and obtain the minimum tripping time. The proposed CIGRE network is a 14-bus feeder DN, and the grid specifics are outlined in [40, 41]. In general, the CIGRE network is operated with an HV/MV utility source and equipped with two PV farms rated 10 MW/each through a setup transformer rated 0.4/12.49 kV, as detailed in [1, 41]. The 10 MW farms include ten of the 1 MW PV systems as described in Section 4.1. The CIGRE network is protected by 12 MFOCRs, where each

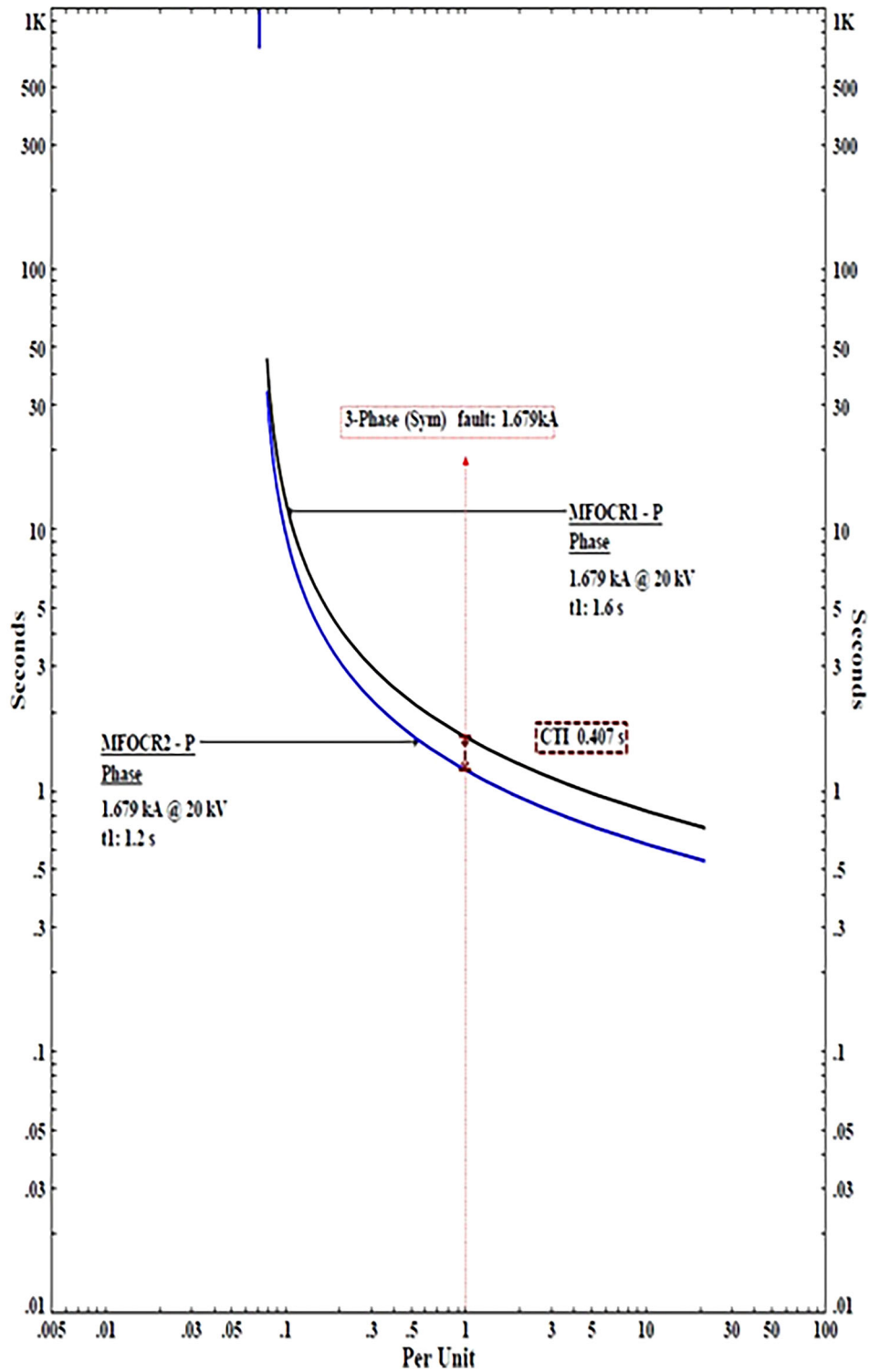


FIGURE 11 The time-current characteristics curves of multifunction overcurrent relays (1 and 2) when three phase fault occurs at location F4 for scenario 1.

fault location from F1 to F12 is assigned two primary MFOCRs and one backup MFOCR. The LG and LLL faults and the locations of the faults (from F1 to F12) represent the near- and far end fault locations from the sources.

In this work, a set of 12 diverse fault locations within the CIGRE 14 bus system are considered. These fault locations

were strategically chosen to cover all the main buses in the system and thoroughly assess the effectiveness of the proposed scheme under various operating conditions and fault scenarios. The basic information of the MFOCRs at the CIGRE network as presented in Figure 10 is described in Table 6 for sub function OF1 and OF2 for phase and ground events, respectively.

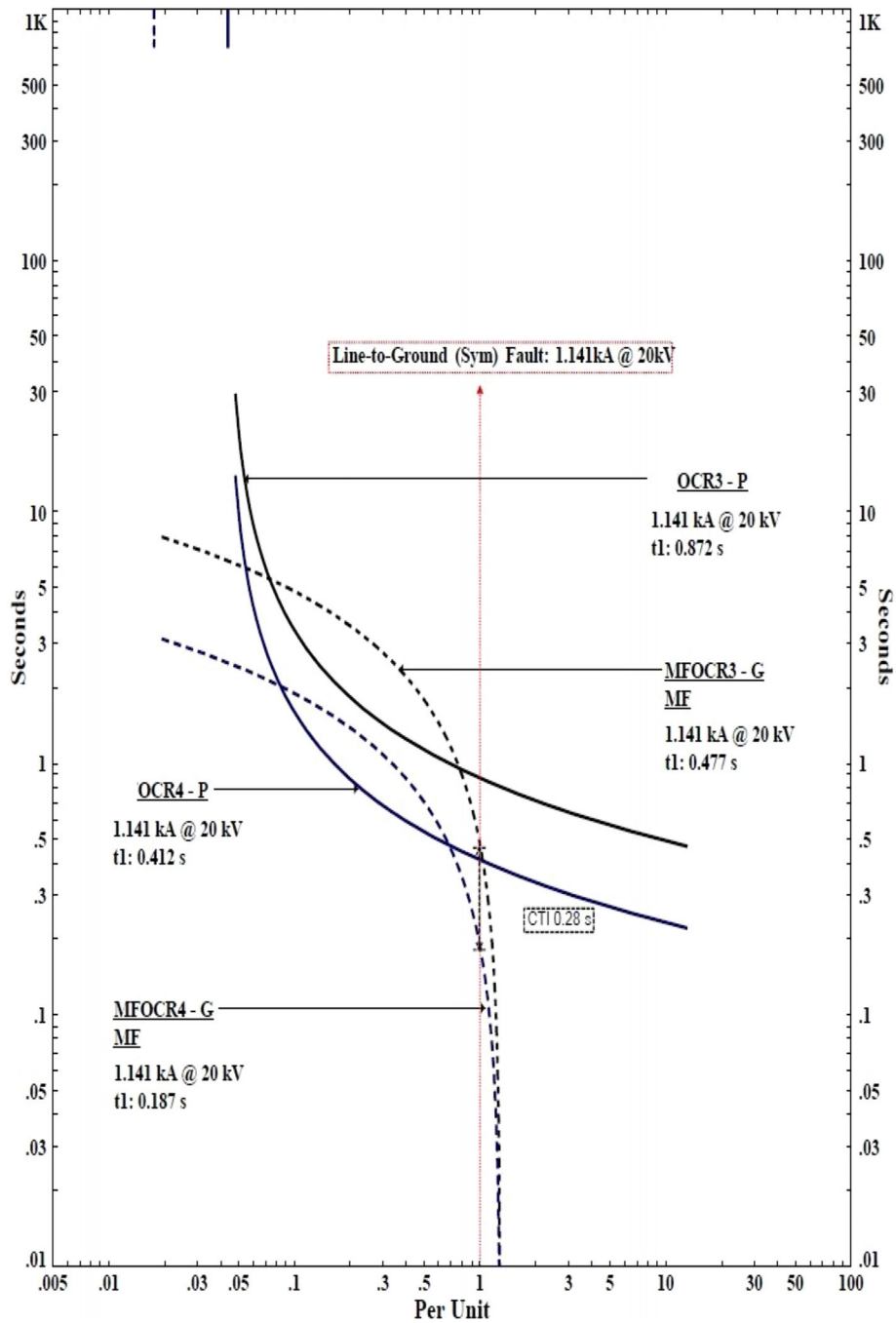


FIGURE 12 The time-current curves of multifunction overcurrent relays (3, 4) and traditional overcurrent (3 and 4) when line to ground fault occurs at location F2 for scenario 1.

Initially, the load flow and faults calculations were generated to establish the current transformer ratio and pickup current for each MFOCR in accordance with IEC-60909.

5.2 | Numerical results

The results of the proposed optimal multifunction protection scheme and standard schemes are presented under various fault and DN operation models. This section com-

pares the performance of the MFOCR coordinating scheme for DN using the CSS algorithms with the following DN configurations:

- Scenario 1: The CIGRE network is powered only by a main HV/MV utility feeder, as shown in Figure 10, to evaluate the proposed optimal multifunction protection scheme on a traditional DN without DGs.
- Scenario 2: The CIGRE network is powered by a main HV/MV utility feeder and two 5 MVA PV farms, as shown

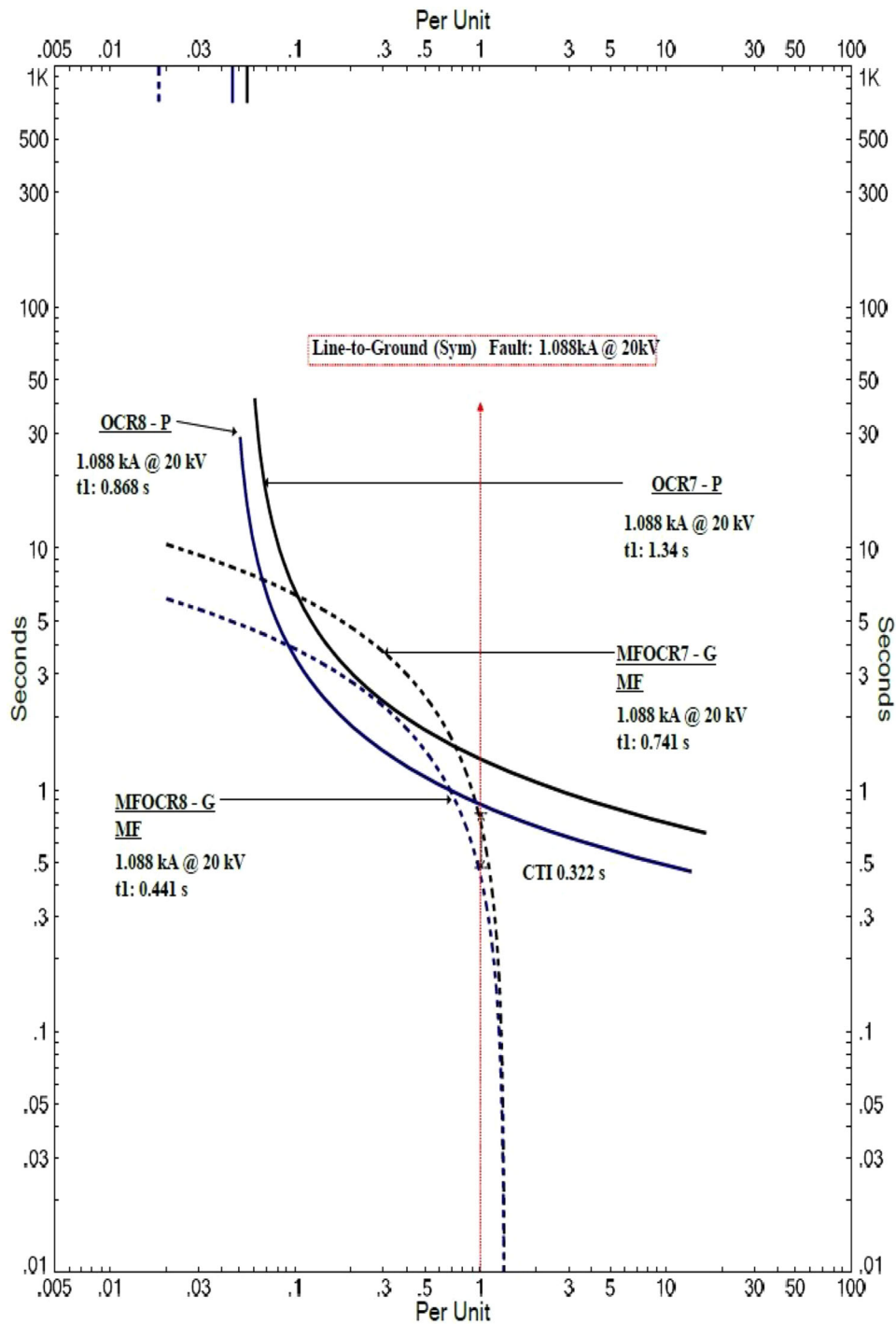


FIGURE 13 The time-current curves of multifunction overcurrent relays (7 and 8) and traditional overcurrent (7 and 8) when line to ground fault occurs at location F7 for scenario 1.

in Figure 10, to investigate the proposed MFOCR scheme in a modern DN with DGs. As described in Section 2, the addition of DGs to the DN complicates the achievement of optimal coordination of OCRs.

- Scenario 3: The CIGRE network will be operated in islanding mode. In the islanding mode, isolated sections of the DN are kept alive by PV systems even in the presence of internal faults. The proposed optimal multifunction protec-

tion scheme works to minimize the total tripping time and increase the selectivity of tripping and of power continuity the healthy lines which will increase the stability DN.

In this work, the proposed multi-OF scheme, as described by multi-OF in Equation (4), based on the time-current characteristics of standard (OF1) and non-standard (OF2) is employed to improve the selectivity and sensitivity of the OCR

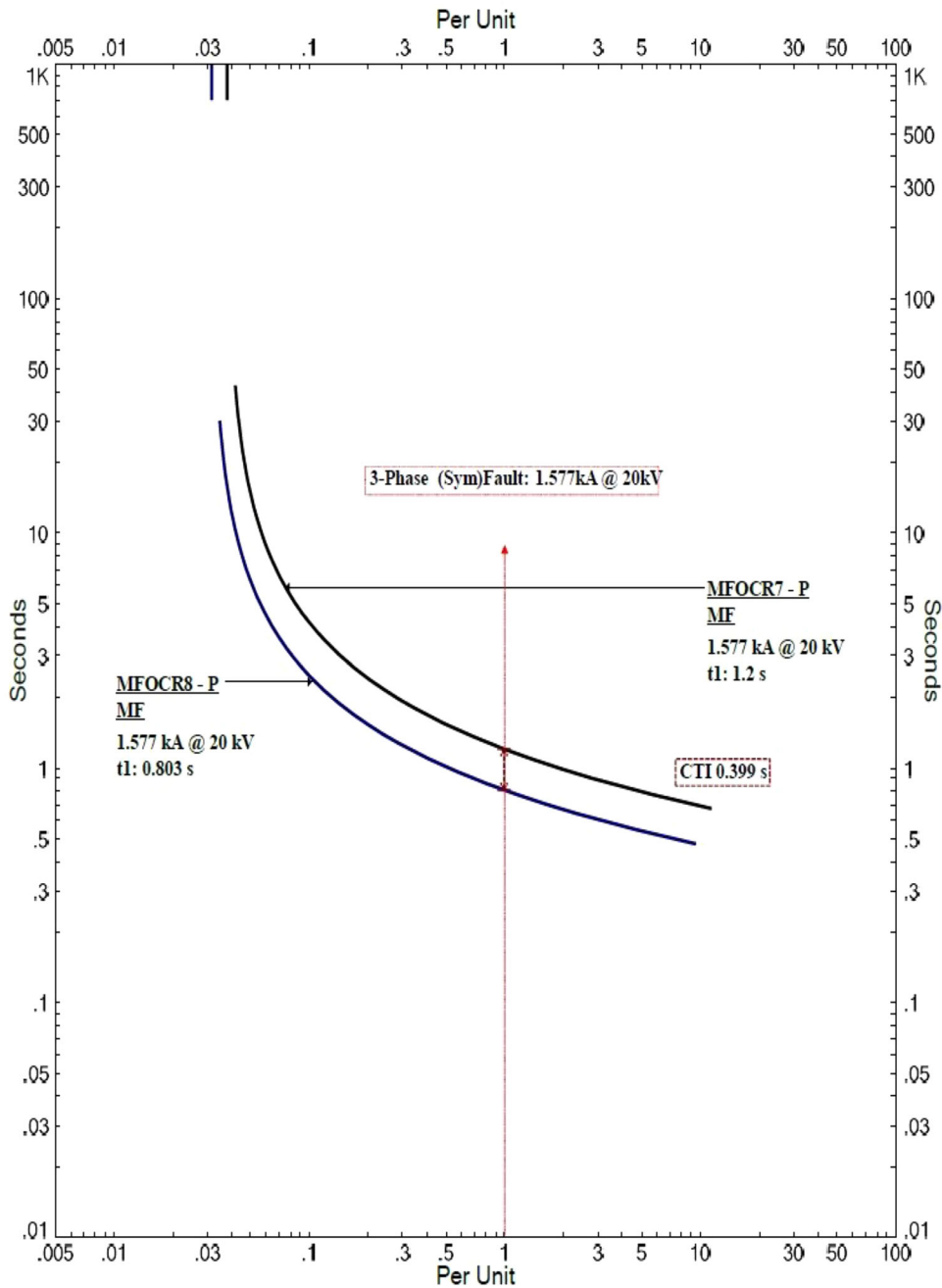


FIGURE 14 The time–current characteristics curves of multifunction overcurrent relays (7 and 8) when three phase fault occurs at location F7 for scenario 2.

protection system. The multi-OF scheme is subjected to protection and network constraints for CTI and TMS, as described in Section 3.1. Table 7 shows the optimal TMS values for OF1 (TMSP, phase OCR sub function) and OF2 (TMSG, ground OCR sub function) in the MFOCRs at the CIGRE network. The TMSP and TMSG for each OCR are optimality calculated according to the maximum load currents in line and different fault scenarios (LLL and LG faults). In this section, to make sure that the primary MFOCRs operate quickly as possible for both sub functions for TWO and CSS methods, the CTI is assumed to be 0.4 and 0.3 s for phase fault mode (OF1) and

ground fault mode (OF2), respectively. Furthermore, the pickup current will be 1.2 and 0.2 from the full load for OF1 and OF2, respectively.

5.2.1 | Scenario 1 test results

In this case, phase and ground faults scenarios are simulated to evaluate the proposed MFOCR scheme in the DN without DG. Firstly, the phase faults (LLL and LL) under OF1 is applied to evaluate the ability of MFOCR to deal with the maximum fault

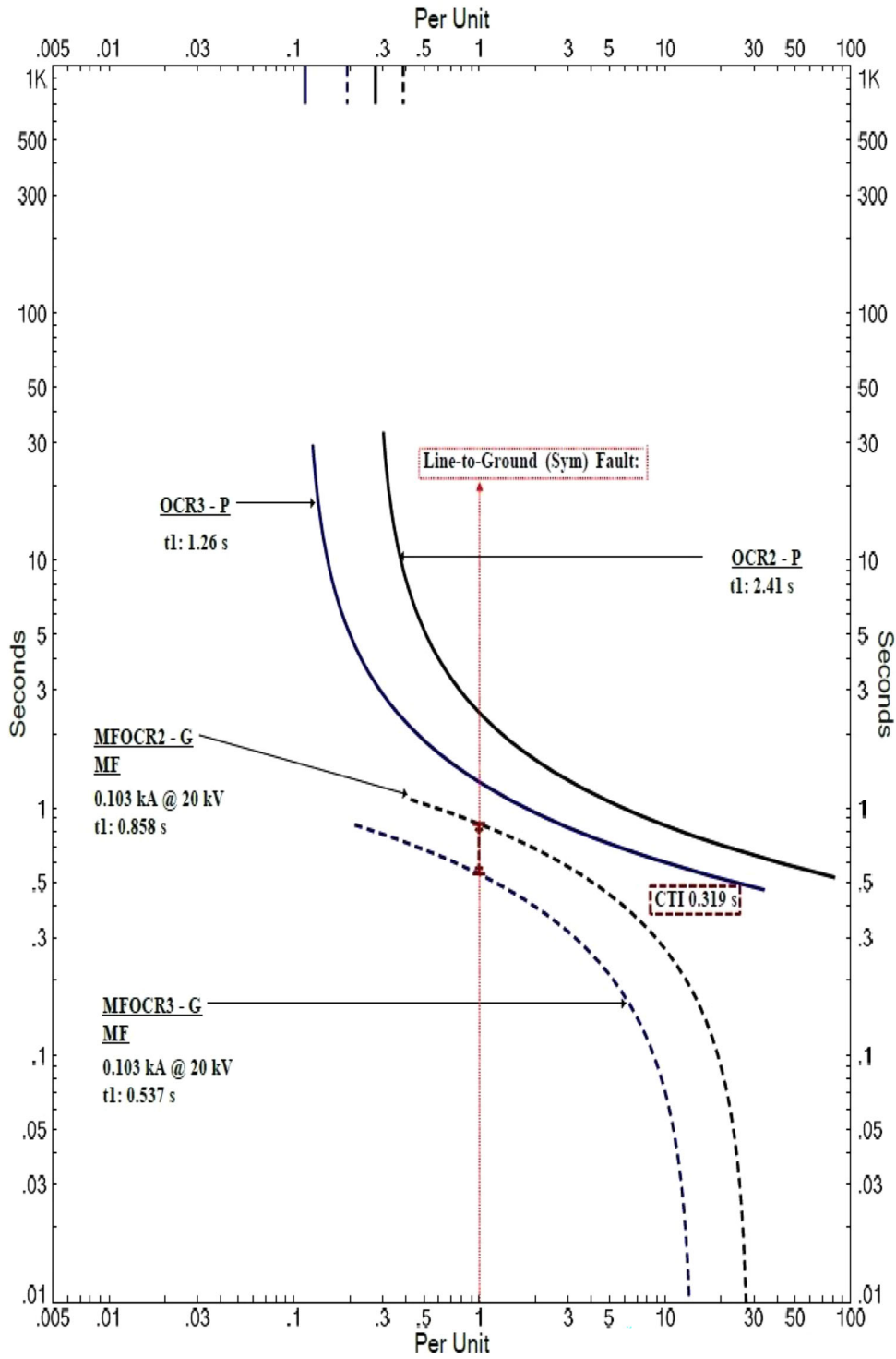


FIGURE 15 The time–current characteristics curves of multifunction overcurrent relays (2 and 3) and traditional overcurrent (2 and 3) when line to ground fault occurs at location F2 for scenario 2.

scenarios as in [4, 16] for single function phase OCR. Table 8 shows the 12 fault location scenarios, fault current values and the recorded tripping time for each relay. For example, MFOCR 5 at F1 (LLL) operated within 0.04 s as the primary relay and MFOCR 4 operated within 0.4 s as the backup relay. This shows that the MFOCRs operated very quickly for primary relays and were complacent with the CTI for backup relays. In addition,

the results of the time tripping of MFOCRs at LLL and LL fault using ETAP software have shown a significant sign of the ability of the MFOCRs to sensitivity work. Figure 11 shows that MFOCR 2 operates for phase fault equal to 1.679 KA (F4) at 1.2 s and MFOCR 1 operates at 1.6 s after a CTI equal to 0.4 s.

Secondly, the ground faults under OF2 is applied to assess the ability of MFOCR with a non-standard curve (OF2) to

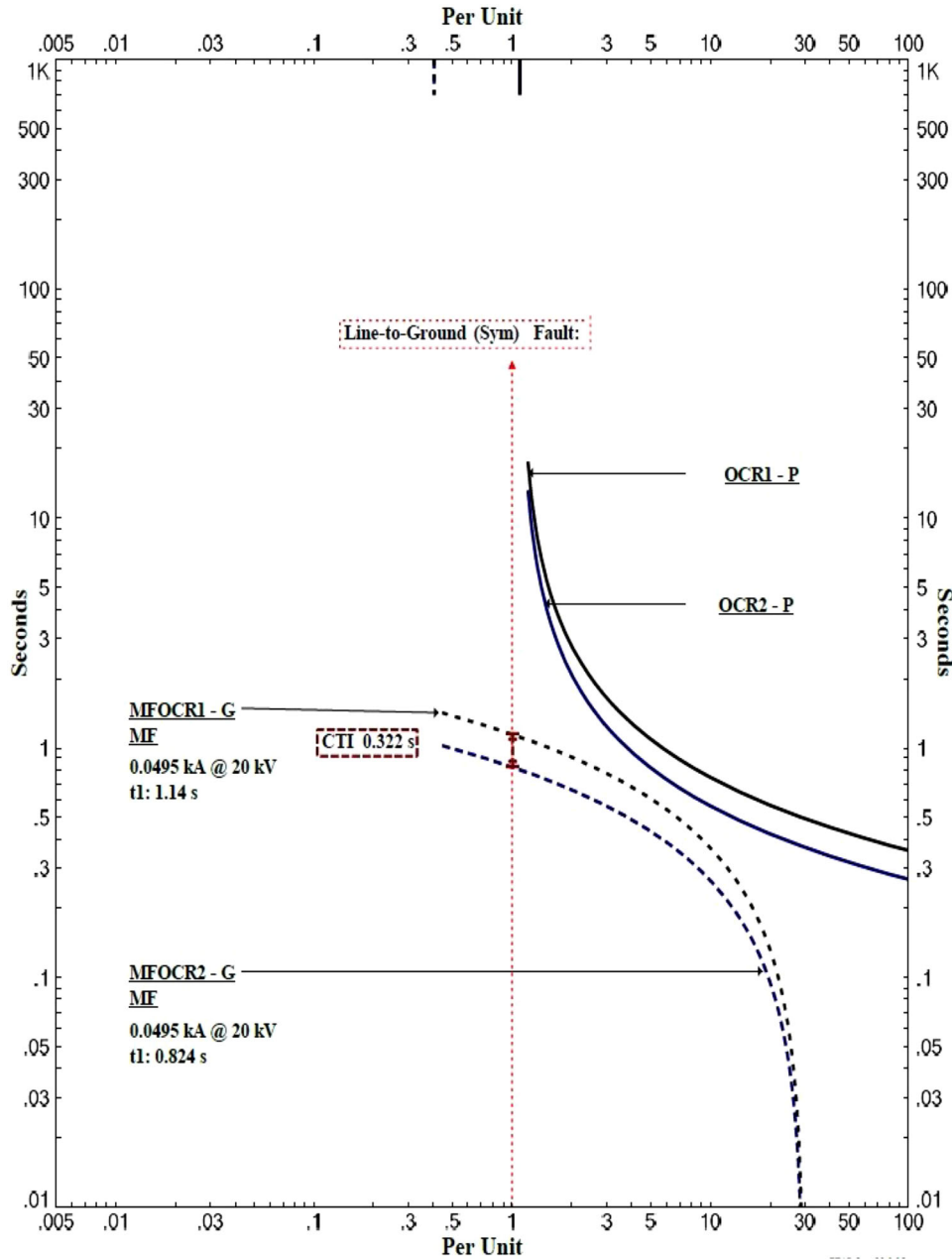


FIGURE 16 The time-current characteristics curves of multifunction overcurrent relays (2 and 3) and traditional overcurrent (2 and 3) when line to ground fault occurs at location F2 for scenario 2.

deal with the ground scenarios compared to the traditional OCR scheme (single function phase OCR) in [16]. Table 9 shows the ground faults (LG and LLG) values and location scenarios, and the recorded tripping time for each relay for MFOCR and traditional OCR scheme. For example, MFOCR 3 at F3 (LG) operated within 0.362 s as the primary relay and MFOCR 2 operated in 0.66 s as a backup relay; while the traditional OCR scheme [16] operated within 0.85 and 1.37 s for primary and backup relays, respectively. This shows that the MFOCRs outperformed the traditional ORC scheme in terms of tripping time under both faults scenarios LG and LLG. The graphical results of the time tripping of MFOCRs and traditional OCR at LG fault using ETAP software are

presented in Figures 12 and 13. The time-current characteristics curves of relays (MFOCR3, MFOCR4, OCR3 and OCR4) under the LG fault occurring at location F2 for scenario 1 are shown in Figure 12. In fault scenario, F7, the primary and backup MFOCRs are operated before the traditional OCR scheme which provides higher sensitivity, as shown in Figure 13.

5.2.2 | Scenario 2 test results

In this section, the impact of the DG (two PV farms) in the DN on the proposed protection schemes is investigated.

TABLE 8 The operational time of the multifunction overcurrent relay at the CIGRE network for three phase and phase to phase faults, scenario 1.

Fault Location	Relay	LLL		LL	
		Fault current	MFOCR	Fault current	MFOCR
F1	MFOCR5	1281.0	0.04	1088.9	0.04
F1	MFOCR4	1281.0	0.4	1088.9	0.45
F2	MFOCR4	1481.0	0.41	1258.9	0.43
F2	MFOCR3	1481.0	0.82	1258.9	0.87
F3	MFOCR3	1571.0	0.81	1335.4	0.85
F3	MFOCR2	1571.0	1.23	1335.4	1.31
F4	MFOCR2	1679.0	1.19	1427.2	1.27
F4	MFOCR1	1679.0	1.62	1427.2	1.73
F5	MFOCR1	3393.0	1.27	2884.1	1.34
F5	—	3463.0	0.02	2943.6	0.02
F6	MFOCR7	1461.0	1.21	1241.9	1.28
F6	MFOCR2	1461.0	1.26	1241.9	1.35
F7	MFOCR8	1415.0	0.80	1202.8	0.84
F7	MFOCR7	1415.0	1.22	1202.8	1.29
F8	MFOCR9	1317.0	0.41	1119.5	0.44
F8	MFOCR8	1317.0	0.82	1119.5	0.86
F9	MFOCR10	1261.0	0.02	1071.9	0.02
F9	MFOCR9	1261.0	0.42	1071.9	0.44
F10	MFOCR6	1251.0	0.07	1063.4	0.08
F10	MFOCR7	1251.0	1.20	1063.4	1.27
F11	MFOCR11	2136.0	0.11	1815.6	0.11
F11	MFOCR12	2136.0	0.52	1815.6	0.54
F12	MFOCR12	3083.0	0.47	2620.6	0.49
F12	—	2943.0	0.04	2501.6	0.00

The LLL and LG faults scenarios are simulated to evaluate the proposed MFOCR scheme compared to the traditional OCR scheme [4]. Figure 14 shows the results of the time tripping of MFOCRs at LLL fault. The ETAP results for the tripping curves of MFOCR introduced a substantial sign of the sensitivity of MFOCRs for phase faults. The MFOCR 8, primary relay, operated for phase fault (F7) at 0.803 s and the MFOCR 7, backup relay, operated at 1.2 s after a CTI equal to 0.399 s. The DGs changed the behaviour and characteristics of faults and increased the complexity of handling ground faults. Table 10 shows the ground faults (LG and LLG) values and location scenarios and the recorded tripping time for each relay for MFOCR and the traditional OCR scheme. The traditional OCR scheme needs more time for primary and backup relays to operate compared to MFOCRs for both fault scenarios (LG and LLG). For example, the MFOCR 4 at F2 (LG) operated within 0.23 s as the primary relay and MFOCR 3 operated within 0.54 s as the backup relay; while the traditional OCR scheme [4, 16] operated within 0.48 and 1.2 s for the primary and backup relay, respectively. This showed that the MFOCRs for both primary and backup relays

TABLE 9 The operational time of the multifunction overcurrent relays and traditional overcurrent relays at the CIGRE network for line to ground and line to line to ground fault, scenario 1.

Fault location	Fault current	Relay	Traditional OCR scheme	MFOCR scheme
LG fault				
F1	981.0	5	0.022	0.005
F1	981.0	4	0.43	0.29
F2	1141.0	4	0.41	0.18
F2	1141.0	3	0.87	0.47
F3	1213.0	3	0.85	0.362
F3	1213.0	2	1.37	0.66
F4	1300.0	2	1.32	0.42
F4	1300.0	1	1.77	0.73
F5	2768.0	1	1.34	0.1
F6	1124.0	7	1.32	0.66
F6	1124.0	2	1.42	0.92
F7	1088.0	8	0.86	0.44
F7	1088.0	7	1.34	0.74
F8	1001.0	9	0.45	0.268
F8	1001.0	8	0.89	0.551
F9	965.0	10	0.023	0.01
F9	965.0	9	0.45	0.30
F10	958.0	6	0.05	0.01
F10	958.0	7	1.4	1.06
F11	1446.0	11	0.02	0.01
F11	1446.0	12	0.342	0.3
F12	2142.0	12	0.3	0.01
LLG fault				
F1	784.0	5	0.04	0.02
F1	784.0	4	0.50	0.40
F2	912.8	4	0.48	0.37
F2	912.8	3	0.97	0.71
F3	970.4	3	0.95	0.70
F3	970.4	2	1.52	1.10
F4	1040.0	2	1.47	1.07
F4	1040.0	1	1.99	1.43
F5	2214.4	1	1.46	1.05
F6	2591.2	7	0.02	0.02
F6	899.2	2	1.43	1.09
F7	899.2	8	1.57	1.14
F7	870.4	7	0.94	0.74
F8	870.4	9	1.45	1.10
F8	800.8	8	0.49	0.40
F9	800.8	10	0.97	0.76
F9	772.0	9	0.02	0.04
F10	772.0	6	0.50	0.41
F10	766.4	7	0.09	0.06
F11	766.4	11	1.42	0.04
F11	1156.8	12	0.13	0.04
F12	1156.8	12	0.62	0.01

TABLE 10 The operational time of the multifunction overcurrent relays and traditional overcurrent relays at the CIGRE network for line to ground fault, scenario 2.

Fault location	Fault current	Relay	Traditional OCR scheme	MFOCR scheme
LG				
F1	876.0	5	0.023	0.007
F1	876.0	4	0.449	0.293
F2	973.0	4	0.48	0.23
F2	99.0	3	1.2	0.54
F3	103.0	3	0.85	0.537
F3	103.0	2	1.37	0.858
F4	164.0	2	2.32	0.74
F4	164.0	1	3.1	1.09
F5	673.0	1	1.34	0.1
F6	922	7	1.45	0.76
F6	150	2	2.54	0.79
F7	902	8	0.96	0.52
F7	902.0	7	1.46	0.83
F8	857	9	0.5	0.28
F8	857.0	8	0.98	0.57
F9	830	10	0.024	0.01
F9	830.0	9	0.45	0.30
F10	830.0	6	0.05	0.01
F10	826.0	7	1.4	1.06
F11	937	11	0.02	0.01
F11	1446.0	12	0.342	0.3
F12	2142.0	12	0.3	0.01
LLG fault				
F1	700.8	5	0.005	0.007
F1	700.8	4	0.407	0.29
F2	778.4	4	0.141	0.23
F2	79.2	3	1.076	0.54
F3	82.4	3	0.669	0.52
F3	82.4	2	1.196	0.858
F4	131.2	2	1.065	0.74
F4	131.2	1	1.632	1
F5	538.4	1	1.058	0.1
F6	737.6	7	0.000	0.76
F6	120	2	0.936	0.7
F7	721.6	8	0.745	0.52
F7	721.6	7	0.268	0.8
F8	685.6	9	0.646	0.28
F8	685.6	8	0.292	0.57
F9	664	10	0.714	0.01
F9	664	9	0.002	0.30
F10	664	6	0.407	0.01
F10	660.8	7	0.008	1.06
F11	749.6	11	0.784	0.006
F11	112.8	12	0.015	0.31
F12	112.8	12	1.503	0.29

TABLE 11 The operational time of the multifunction overcurrent relays and traditional overcurrent relays at the CIGRE network for line to ground fault, scenario 3.

Fault location	Fault current	Relay	Traditional OCR scheme	MFOCR scheme
F3	31.0	3	1.97	0.63
F3	31.0	2	No trip	0.93
F4	49.0	2	No trip	0.82
F4	49.0	1	No trip	1.14
F11	300.0	11	0.02	0.01
F11	302.0	12	0.97	0.32
F12	46.0	12	0.3	0.01

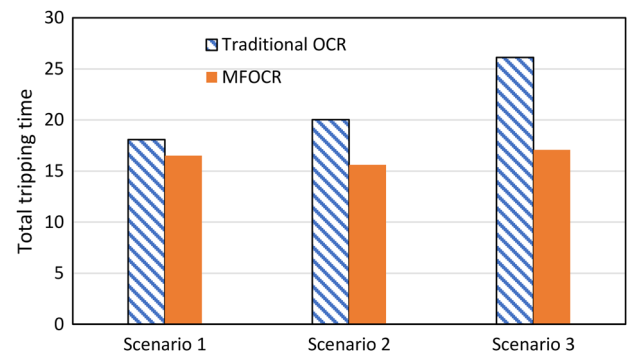


FIGURE 17 Total tripping time for multifunction overcurrent relays and traditional overcurrent relays schemes over different grid operation scenarios.

outperformed the traditional ORC scheme in terms of tripping time. For example, the graphical results of time-current characteristics curves of relays (MFOCR2, MFOCR3, OCR2 and OCR3) under the LG fault occur at location F2 for scenario 2 are shown in Figure 15. In fault scenario, F2, the primary and backup MFOCRs are operated before the traditional OCR scheme which provides higher sensitivity.

5.2.3 | Scenario 3 test results: DN with DGs operates in islanding mode

The performance of the MFOCR scheme is examined on the DN with DGs shown in Figure 10 under the islanding mode operation (Scenario 3). As the 10 MW PV systems are connected to Bus 4 and Bus 13, the operational time for MFOCRs and traditional OCR at F3, F4, F11 and F12 with LG fault condition is presented in Table 11. In this scenario, the MFORC during F3 operated at 0.63 and 0.93 s for primary and backup relays, respectively, while the OCR operated at 1.97 s for the primary relay and the backup did not operate. The traditional OCR scheme did not act as a primary or backup relay for relays 2 and 5 during F4 faults, as shown in Figure 16. The MFOCR approach showed better performance during F4 faults with a tripping time of 0.82 and 1.14 s for the primary and backup relays, respectively.

TABLE 12 The total tripping time of the MFOCRs using the Tug of War, Charged System Search and Particle Swarm optimization algorithms under different fault and grid mode scenarios.

Grid operation mode	Scenario 1			Scenario 2			Scenario 3											
	LLL	LG	LG	LLL	LG	LG	LLL	LG	LG									
Fault scenario	TWO	PSO	PSO	TWO	PSO	PSO	TWO	PSO	PSO									
	18.62	16.19	26.8	18.08	16.5	19.11	13.58	12.38	14.0									
	16.19	16.5	19.11	13.58	12.38	14.0	20.07	15.61	22.2									
Optimization algorithm	TWO	CSS	PSO	TWO	CSS	PSO	TWO	CSS	PSO									
	18.62	16.19	26.8	18.08	16.5	19.11	13.58	12.38	14.0									
	16.19	16.5	19.11	13.58	12.38	14.0	20.07	15.61	22.2									
Total tripping time	18.62	16.19	26.8	18.08	16.5	19.11	13.58	12.38	14.0	20.07	15.61	22.2	18.18	15.43	19.3	26.11	17.07	26.3

5.3 | Discussion and comparison

This section investigates and presents the performance of the suggested MFOCR approach compared to the traditional OCR strategy in three scenarios of power grids (with and without PV and islanding mode). Figure 17 displays the total tripping times for the relays under the LG faults for the three grid operation scenarios. The total tripping time for each scenario was computed using the CSS optimization technique for the MFOCR and traditional OCR strategy approaches. The proposed MFOCR approach outperformed the traditional OCR scheme in all scenarios. The MFOCR reduced the total tripping time by 8.8%, 22.1% and 34.6% compared to the traditional OCR scheme for scenarios 1 to 3, respectively, as shown in Figure 17. The results show that the islanding mode is highly complex to be detected compared to other scenarios and the proposed MFOCR successfully reduced the tripping time for this scenario without any non-tripping events.

5.3.1 | ORCs coordination based on different optimization algorithms

In this subsection, the performance of the proposed MFOCR scheme using TWO and CSS optimization methods is presented and compared to particle swarm optimization (PSO) algorithm as common and traditional optimization algorithm for solving power system problems [16]. Table 12 demonstrates the total tripping time under different fault and grid mode scenarios. The results show that the CSS algorithm is preferable to the three grid operation scenarios in terms of reducing the total tripping during the LLL and LG fault scenarios. For instance, the CSS algorithm reduced the total tripping time during the LG and LLL events at scenario 2 to 15.61 and 12.38 s, respectively, compared to the TWO models with 20.07 and 13.58 s. As shown in Table 10, both proposed algorithms (TWO and CSS) outperformed the PSO algorithm over the three power network operation scenarios.

To examine the performance of the TWO, CSS and PSO algorithms in terms of convergence rate and stability. Figures 18 and 19 display the convergence curves for the TWO, CSS and PSO algorithms under LLL and LG fault scenarios at islanding and without PV operation modes. First, Figure 18 demonstrates the performance of the optimization algorithms under LG fault, scenario 3. The CSS algorithm had a smoother convergence curve and achieved optimal results very quickly with fewer iterations compared to TWO and PSO. Figure 19 shows the performance of the optimization method under LLL fault and scenario 1. In this scenario, the CSS and TWO with similar performance outperformed the PSO in terms of convergence rate and stability. This shows that the CSS had lower computation costs and smoother convergence compared to TWO and PSO which help in improving the CPU utilization efficiency. In this work, the maximum number of iterations is selected as the termination condition for the optimization algorithms similar to the literature [16, 36]. The maximum number of

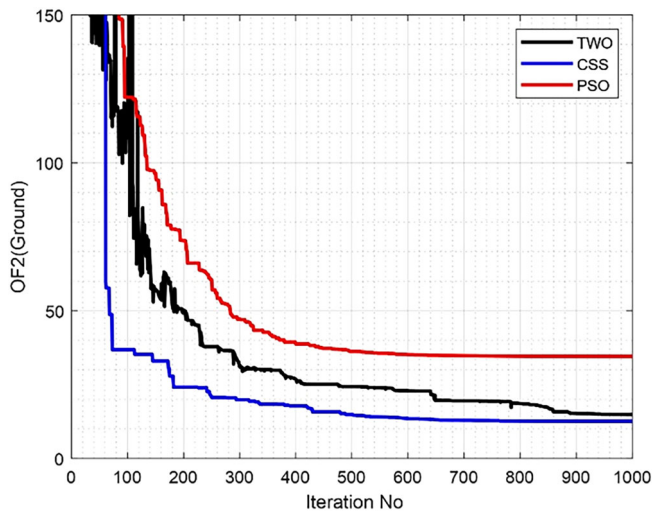


FIGURE 18 The convergence curves for the CSS, TWO and PSO optimization algorithms under LG fault, scenario 3.

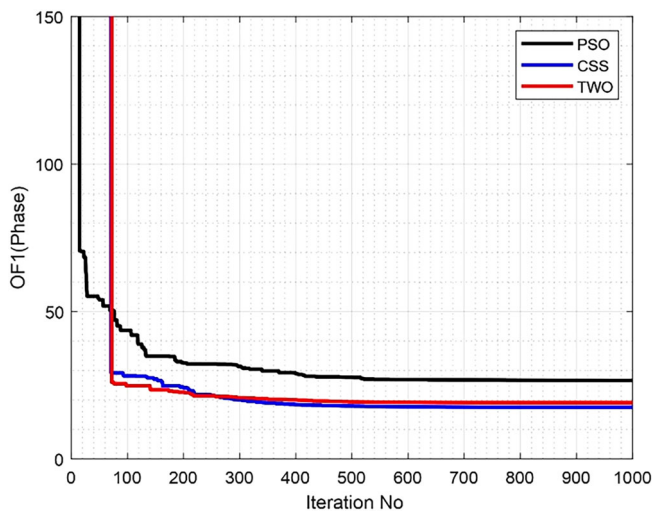


FIGURE 19 The convergence curves for the Tug of War, Charged System Search and Particle Swarm optimization algorithms under three phase fault, scenario 1.

iterations is chosen in this work by performing experimentation and analysis to determine the suitable value for the proposed optimization problem in this work. This approach helps find a balance between exploring the search area enough, finding optimal results, providing opportunity for convergence and preventing excessive computational time.

6 | CONCLUSIONS AND RECOMMENDATIONS

The main purpose of this research is to introduce a sensitive and fast OCR protection scheme for different power and fault network architecture. The OCR coordination problem is formulated as a multifunction problem for phase and ground faults.

Regardless of the operating conditions (with and without PV and islanding mode), the proposed MFOCR strategy reduces the total tripping time and outperforms the traditional OCR scheme. The proposed MFOCR approach is formulated and solved using CSS and TWO algorithms to achieve the optimal settings during different fault and grid operation scenarios. In addition, this research aims to provide a novel and straightforward protection strategy for use in DN with DGs during ground fault scenarios. The results of the proposed MFOCR approach completed the coordination task successfully and achieved the minimum tripping time in the three DN operational scenarios. The MFOCR reduced the total tripping time by 8.8%, 22.1% and 34.6% compared to the traditional OCR scheme for scenarios 1 to 3, respectively. This showed that the traditional phase OCR is not suitable to be the primary protection for ground faults. Moreover, the CSS and TWO optimization techniques were compared to find a fast trip time solution, where the CSS outperformed TWO in terms of tripping time and convergence rate. Machine learning methods will be needed in the future to reduce tripping time and increase protection selectivity performance.

NOMENCLATURE

DGs	Distribution generators
OF	Objective function
OCRs	Over current relays
LL	Line to line fault
TWO	Tug of war optimization algorithm
CSS	Charged system search algorithm
CTI	Coordination time interval
GA	Genetic algorithm
SQP	Sequential quadratic programming
PSO	Particle swarm optimization
DN	Distribution network
GWO	Grey wolf optimizer
GA-LP	Genetic algorithm-linear programming
EP	Evolutionary programming
TLBO	Teaching learning-based optimization
PSA	Pattern search algorithm
MFA	Modified firefly algorithm
IPM	Interior point method
NSGA-II	Non-dominated sorting genetic algorithm-II
FBGA	Fuzzy logic-genetic algorithm
MOPSO/FDMT	Multi-objective particle swarm optimization/ fuzzy decision-making tool
IWO	Invasive weed optimization algorithm
DEA	Differential evolution algorithm
PVs	Photovoltaic systems
LLL	Three phase faults
LG	Line to ground fault
LLG	Line-line to ground fault
TMS	Multiplier settings
t_{prim}	Tripping time of primary relay
t_{back}	Tripping time of backup relay

I_f	Fault current
I_{pick}	Pickup current
$\sum f_c$	Fault current limiter
TMSP	TMS for phase OCR function
TMSG	TMS for ground OCR function
t_g	Tripping time at ground function
t_p	Tripping time at phase function
MFOCR	Multifunction protection scheme for phase and ground OCRs
DE/LP	Differential Evolution- Linear Programming
ESA-DEMO	Enhanced self-adaptive differential evolution multi-objective
FAGAM	Fmincon function and goal attainment method.
ER-WCA	Evaporation rate water cycle algorithm
MO-SSA-LP	
MRFO	Manta ray foraging optimization
NSGA-II-MILP	Non-dominated sort genetic algorithm-mixed integer linear problem
GA-PSO-LP	Genetic algorithm-particle swarm optimization-linear programming

AUTHOR CONTRIBUTIONS

Feras M. Alasali: Conceptualization; Formal analysis; Funding acquisition; Investigation; Methodology; Project administration; Software; Validation; Writing—original draft. Naser Naili: Conceptualization, Data curation, Investigation, Methodology, Resources, Software, Writing—original draft. Abdelaziz Salah Saidi: Methodology; Project administration; Software; Supervision; Validation; Writing—review and editing. Awni Itradat: Formal analysis; Investigation; Methodology; Supervision; Validation; Writing—review and editing. William Holderbaum: Formal analysis; Methodology; Project administration; Software; Supervision; Validation; Visualization; Writing—review and editing. Faisal Mohamed: Conceptualization, Data curation, Investigation, Project administration, Software, Validation, Writing—review and editing.

ACKNOWLEDGEMENTS

The authors would like to thank the University of Salford and The Hashemite University (Renewable Energy Center) for their support in publishing this article. The authors extend their appreciation to the Deanship of Scientific Research at King Khalid University for funding this work through large group Research Project under grant number: RGP2/85/44.

CONFLICTS OF INTEREST STATEMENT

The authors declare no conflicts of interest.

DATA AVAILABILITY STATEMENT

Not applicable.

ORCID

Feras Alasali  <https://orcid.org/0000-0002-1413-059X>

REFERENCES

- Alasali, F., El-Naily, N., Zarour, E., Saad, S.M.: Highly sensitive and fast microgrid protection using optimal coordination scheme and nonstandard tripping characteristics. *Int. J. Electr. Power Energy Syst.* 128, 106756 (2021)
- Patnaik, B., Mishra, M., Bansal, R.C., Jena, R.K.: AC microgrid protection_A review: Current and future prospective. *Appl. Energy* 271, 115210 (2020)
- Alasali, F., Zarour, E., Holderbaum, W., Nusair, K.: Highly sensitive and fast microgrid protection using optimal coordination scheme and nonstandard tripping characteristics. *Int. J. Electr. Power Energy Syst.* 128, 106756 (2021)
- So, C.W., Li, K.K., Lai, K.T., Fun, K.Y.: Application of genetic algorithm for overcurrent relay coordination. In: *Sixth International Conference on Developments in Power System Protection (Conf. Publ. No. 434)*. Nottingham, UK (1997). <https://doi.org/10.1049/cp:19970030>
- So, C.W., Li, K.K.: Overcurrent relay coordination by evolutionary programming. *Electr. Power Syst. Res.* 53, 83–90 (2000)
- Birla, D., Maheshwari, R., Gupta, H.: A new nonlinear directional overcurrent relay coordination technique, and banes and boons of near-end faults based approach. *IEEE Trans. Power Delivery* 21(3), 1176–1182 (2006)
- Razavi, F., Abyaneh, H., Al-Dabbagh, M., Mohammadi, R., Torkaman, H.: A new comprehensive genetic algorithm method for optimal overcurrent relays coordination. *Electr. Power Syst. Res.* 78, 713–720 (2008)
- Mohammadi, R., Abyaneh, H., Razavi, F., Al-Dabbagh, M., Sadeghi, S.: Optimal relays coordination efficient method in interconnected power systems. *J. Electr. Eng.* 61(2), 75–83 (2010)
- Mohammadi, R., Abyaneh, H., Rudsari, H., Fathi, S., Rastegar, H.: Overcurrent relays coordination considering the priority of constraints. *IEEE Trans. Power Delivery* 26(3), 1927 (2011)
- Singh, M., Panigrahi, B., Abhyankar, A.: Optimal coordination of directional over-current relays using teaching learning-based optimisation (TLBO) algorithm. *Int. J. Electr. Power Energy Syst.* 50, 33–41 (2013)
- Mosavi, S., Kejani, T., Javadi, H.: Optimal setting of directional overcurrent relays in distribution networks considering transient stability. *Int. Trans. Electr. Energy Syst.* 26(1), 122–133 (2015). <https://doi.org/10.1002/etep.2072>
- Hussain, M., Hussain, I., Abidin, A., Rahim, S.: Multi-objective approach for solving directional overcurrent relay problem using modified firefly algorithm. *Int. J. Comput. Commun. Instrum. Eng.* 3, 21–26 (2016)
- Alam, M., Pnat, B.: An interior point method based protection coordination scheme for directional overcurrent relays in meshed networks. *Int. J. Electr. Power Energy Syst.* 81, 153–164 (2016)
- Moravej, Z., Adelnia, F., Abbasi, F.: Optimal coordination of directional overcurrent relays using NSGA-II. *Electr. Power Syst. Res.* 119, 228–236 (2015)
- Alkaran, D., Vatani, M., Sanjari, M., Gharehpetian, G., Naderi, M.: Optimal overcurrent relay coordination in interconnected networks by using fuzzy-based GA method. *IEEE Trans. Smart Grid* 9, 3091–3101 (2018). <https://doi.org/10.1109/TSG.2016.2626393>
- Yazdanejadi, A., Naderi, M., Gharehpetian, G., Talavat, V.: Protection coordination of directional overcurrent relays: New time current characteristic and objective function. *IET Gener. Transm. Distrib.* 12, 190–199 (2018)
- Baghaee, H., Mirsalim, M., Gharehpetian, G., Talebi, H.: MOPSO/FDMT-based Pareto-optimal solution for coordination of overcurrent relays in interconnected networks and multi-DER microgrids. *IET Gener. Transm. Distrib.* 12, 2871–2886 (2018)
- Rajput, V., Adelnia, F., Pandya, K.: Optimal coordination of directional overcurrent relays using improved mathematical formulation. *IET Gener. Transm. Distrib.* 12, 2086–2094 (2018)
- Castillo, C., Conde, A., Shih, M.: Improvement of non-standardized directional overcurrent relay coordination by invasive weed optimisation. *Electr. Power Syst. Res.* 157, 48–58 (2018)
- Sharma, A., Kiran, D., Panigrahi, B.: Planning the coordination of overcurrent relays for distribution systems considering network reconfiguration and load restoration. *IET Gener. Transm. Distrib.* 12, 1672–1679 (2018)

21. Pereira, K., Pereira, B. Jr., Contreras, J., Mantovani, J.: A multi-objective optimisation technique to develop protection systems of distribution networks with distributed generation. *IEEE Trans. Power Syst.* 33, 7064–7075 (2018)
22. Costa, M., Ravetti, M., Saldanha, R., Carrano, E.: Minimizing undesirable load shedding through robust coordination of directional overcurrent relays. *Int. J. Electr. Power Energy Syst.* 113, 748–757 (2019)
23. Shih, M., Conde, A., Ángeles-Camacho, C.: Enhanced self-adaptive differential evolution multi-Objective algorithm for coordination of directional overcurrent relays contemplating maximum and minimum fault points. *IET Gener. Transm. Distrib.* 13, 4842–4852 (2019)
24. Gutierrez, E., Conde, A., Shih, M., Fernández, E.: Execution time enhancement of DOCR coordination algorithms for on-line. *Electr. Power Syst. Res.* 170, 1–12 (2019)
25. Afifi, M., Sharaf, H., Sayed, M., Ibrahim, D.: Comparative study between single-objective and multi-objective optimisation approaches for directional overcurrent relays coordination considering different fault locations. In: *IEEE Milan PowerTech*. Milan, Italy (2019). <https://doi.org/10.1109/PTC.2019.8810815>
26. El-Naily, N., Saad, S., Mohamed, F.: Novel approach for optimum coordination of overcurrent relays to enhance microgrid earth fault protection scheme. *Sustainable Cities Soc.* 54, 102006 (2020). <https://doi.org/10.1016/j.scs.2019.102006>
27. Samadi, A., Chabanloo, R.: Adaptive coordination of overcurrent relays in active distribution networks utilizing a multi-objective optimisation approach. In: *14th International Conference on Protection & Automation in Power System*. Tehran (2020)
28. Sadeghi, M., Dastfan, A., Damchi, Y.: Optimal coordination of directional overcurrent relays in distribution systems with DGs and FCLs considering voltage sag energy index. *Electr. Power Syst. Res.* 191, 106884 (2021). <https://doi.org/10.1016/j.epsr.2020.106884>
29. Akdag, O., Yeroglu, C.: Optimal directional overcurrent relay coordination using MRFO algorithm: A case study of adaptive protection of the distribution network of the Hatay province of Turkey. *Electr. Power Syst. Res.* 192, 106998 (2021). <https://doi.org/10.1016/j.epsr.2020.106998>
30. Sadeghi, M., Dastfan, A., Damchi, Y.: Robust and adaptive coordination approaches for co-optimisation of voltage dip and directional overcurrent relays coordination. *Int. J. Electr. Power Energy Syst.* 129, 106850 (2021). <https://doi.org/10.1016/j.ijepes.2021.106850>
31. Faria, W., Nametala, C., Pereira, B. Jr.: Cost-effectiveness enhancement in distribution networks protection system planning. *IEEE Trans. Power Delivery* 37, 1180–1192 (2022). <https://doi.org/10.1109/TPWRD.2021.3079926>
32. Sadeghi, S., Hashemi-Dezaki, H., Entekhabi-Nooshabadi, A.: Optimized protection coordination of smart grids considering N-1 contingency based on reliability-oriented probability of various topologies. *Electr. Power Syst. Res.* 213, 108737 (2022). <https://doi.org/10.1016/j.epsr.2022.108737>
33. Ataee-Kachoee, A., Hashemi-Dezaki, H., Ketabi, A.: Optimized adaptive protection coordination of microgrids by dual-settingdirectional overcurrent relays considering different topologies based on limited independent relays' setting groups. *Electr. Power Syst. Res.* 214, 108879 (2023). <https://doi.org/10.1016/j.epsr.2022.108879>
34. Usama, M., Mokhlis, H., Mansor, N., Moghavvemi, M., Akhtar, M., Bajwa, A., Awal, L.: A multi-objective optimisation of FCL and DOCR settings to mitigate distributed generations impacts on distribution networks. *Int. J. Electr. Power Energy Syst.* 147, 108827 (2023). <https://doi.org/10.1016/j.ijepes.2022.108827>
35. El-Naily, N., Saad, S., Elhaffar, A., Zarour, E., Alasali, F.: Innovative adaptive protection approach to maximize the security and performance of phase/earth overcurrent relay for microgrid considering earth fault scenarios. *Electr. Power Syst. Res.* 206, 107844 (2022). <https://doi.org/10.1016/j.epsr.2022.107844>
36. Kaveh, A., Bakhshpoori, T.: *Metaheuristics: Outlines, MATLAB Codes and Examples*. Springer Nature Switzerland AG (2019). <https://doi.org/10.1007/978-3-030-04067-3>
37. Miao, X., Zhao, D., Lin, B., Jiang, H., Chen, J.: A differential protection scheme based on improved DTW algorithm for distribution networks with highly-penetrated distributed generation. *IEEE Access* 11, 40399–40411 (2023). <https://doi.org/10.1109/ACCESS.2023.3269298>
38. Chang, N., Song, G., Hou, J., Chang, Z.: Fault identification method based on unified inverse-time characteristic equation for distribution network. *Int. J. Electr. Power Energy Syst.* 146, 108734 (2023)
39. Aramasu, V., Wu, B., Alepuz, S., Kouro, S.: Predictive control for low-voltage ride through enhancement of three-level-boost and NPC-converter-based PMSG wind turbine. *IEEE Trans. Ind. Electron.* 61(12), 6832–6843 (2014)
40. Alasali, F., Saidi, A.S., El-Naily, N., Smadi, M.A., Holderbaum, W.: Hybrid tripping characteristic-based protection coordination scheme for photovoltaic power systems. *Sustainability* 15, 1540 (2023). <https://doi.org/10.3390/su15021540>
41. e-cigre: Benchmark systems for network integration of renewable and distributed energy resources. (2014). https://e-cigre.org/publication/ELT_273_8-benchmark-systems-for-network-integration-of-renewable-and-distributedenergy-resources (accessed on 6 Feb 2023)

How to cite this article: Alasali, F., El-Naily, N., Saidi, A.S., Itradat, A., Holderbaum, W., Mohamed, F.A.: Highly sensitive multifunction protection coordination scheme for improved reliability of power systems with distributed generation (PVs). *IET Renew. Power Gener.* 1–24 (2023). <https://doi.org/10.1049/rpg2.12820>